Final report to the

National Aeronautics and Space Agency (NASA)

for

NASA grant NAG-1-2196

Entitled

"The Continuation of Cloud Statistics for NASA Climate Change Studies"

dates

18 April 1999 – 17 April 2001

from

The University of Wisconsin-Madison
Space Science and Engineering Center
1225 West Dayton Street
Madison, WI 53706

written by

Donald P. Wylie
Principal Investigator
Associate Scientist
Phone 608 263 7458
E-mail don.wylie@ssec.wisc.edu

ACCOMPLISHMENTS:

In finishing the FIRE Arctic Cloud Experiment (FIRE/ACE) two papers were written under this grant; 1) Arctic weather during the FIRE/ACE flights in 1998, and 2) Effects of Long Range Transport and Clouds on Cloud Condensation Nuclei in the Springtime Arctic. The first paper will appear in the FIRE/ACE special issue of Journal of Geophysical Research which is expected to be the June 2001 addition of the journal. The second paper has recently been submitted to JGR. Both papers are included in this report as Appendices A and B.

The first paper discusses the weather events encountered during the FIRE/ACE flights in the spring and summer of 1998. The cyclonic storms, precipitation events, and high pressure systems are chronologically listed. The sources of air reaching the SHEBA ship station in the ice also are discussed. Comparisons are made to other studies of arctic weather and air trajectories to show the similarities and differences of the FIRE/ACE data set from the other studies.

The second paper is co-authored with James Hudson of the Desert Research, Reno Nevada. It discusses the changes in cloud condensation nuclei (CCN) and condensation nuclei (CN) found between the eight flights in May 1998. Back trajectories of the air reaching the SHEBA ship where the data were taken, were examined in detail. James Hudson made the measurements of CCN and CN on the FIRE/ACE flights. The importance of this paper is the study of how the clouds removed CCN and CN from the air causing large changes between FIRE/ACE flights. The FIRE/ACE also provided an opportunity to observe CCN at the levels of cirrus clouds because of the lower altitudes of Ci in the polar atmosphere than in other areas. Ci were found to be poor scavengers of CN and CCN particles. The Arctic data also is compared to CCN and CN data from other locations to show the unique processes in the arctic ocean.

PAPER PUBLISHED:

Wylie, D. P., and Pi-Huan Wang, 1997: Comparison of cloud frequency data from the high-resolution infrared radiometer sounder and the Stratospheric Aerosol and Gas Experiment II., *J. Geophys. Res.*, **102**, 29,893-29,900.

Wylie, D. P., D. Santek, and D. O'C. Starr, 1998: Cloud-top heights from GOES-8 and GOES-9 stereoscopic imagery., *J. Appl. Meteor.*, **37**, 405-413.

Wylie, D. P., and W. P. Menzel, 1999: Eight years of high cloud statistics using HIRS., *J. Climate*, **12**, 170-184.

Wylie, D. P., 2001: Arctic weather during the FIRE/ACE flights in 1998, *J. Geophys. Res.*, in press.

Wylie, D. P., and J. G. Hudson, 2001: Effects of Long Range Transport and Clouds on Cloud Condensation Nuclei in the Springtime Arctic., *Submitted to J. Geophys. Res.*

Appendix A:

Arctic Weather During the FIRE/ACE Flights in 1998

by
Donald P. Wylie

Space Science and Engineering Center
University of Wisconsin-Madison
Madison, WI 54706

Submitted to JGR Atmospheres
December 1999
Accepted November 2000
Scheduled to be published in June 2001

Abstract

The weather systems, cyclones and anticyclones, along with air trajectories and cloud forms, are compared to past studies of the Arctic to assess compatibility of the four month study of FIRE/ACE with past climatologies. The frequency and movement of cyclones (lows) and anticyclones (highs) followed the general eastward and northeastward directions indicated by past studies. Most cyclones (lows) came from eastern Siberia and the Bering Sea to the south and moved north across the Bering Straight or Alaska into the Arctic Ocean. They generally weakened in central pressure as they moved poleward. Anticyclones (highs) were most common in the eastern Beaufort Sea near Canada in June and July as predicted from previous studies. However, many cyclones and anticyclones moved in westward directions which is rare in other latitudes. Erratic changes in shape and intensity on a daily basis also were observed. The NCEP analysis generally reflected the SHEBA Ship WMO observations which it used. However, NCEP temperatures were biased warm by 1.0° to 1.5° C in April and early May. In July when the surface temperature were at the freezing/thawing point, the NCEP analysis changed to a cold bias of -1.0° C. Dew points had smaller biases except for July where they were biased cold by –1.4° C. Wind speeds had a –2 m/s low bias for the six windiest days. Surface barometric pressures had consistently low biases from –1.2 to –2.8 hPa in all four months.

Air parcel historical trajectories were mainly from the south or from local anticyclonic gyres in the Beaufort Sea. Most air came to the SHEBA Ship from the north Pacific Ocean or from Alaska and Canada and occasionally from eastern Siberia. Very few trajectories traced back across the pole to Europe and Central Asia.

Cloud cover was high, as expected, from 69-86% of the time. Satellite data also indicate frequent stratus, altostratus, and cirrus clouds (occurring 61% of the time) above the expected boundary layer fog and Arctic stratus clouds.

1. Introduction

The Arctic Cloud Experiment flights of the First ISCCP Regional Experiment (FIRE/ACE) were held in the spring and summer of 1998 in conjunction with the Surface Heat Budget in the Arctic (SHEBA) program. FIRE/ACE is extensively described by Curry et al. (2000). SHEBA maintained a ship in the Arctic Ocean ice for 13 months from October 1997 to October 1998 while FIRE/ACE flew research aircraft over the SHEBA Ship from 8 April to 29 July 1998.

This paper examines the weather (synoptic events, cloud conditions, and air parcel trajectories) at the SHEBA Ship Ice Camp during the FIRE/ACE research flights. One of the goals of FIRE/ACE was to produce a data set to support numerical modeling of Arctic clouds and radiation for understanding and predicting climate. The SHEBA ship and FIRE/ACE data set is very important because few observations have been taken in the Arctic Ocean. Short duration camps have been made on the ice in previous years and some drifting buoys have been deployed. But no continuous weather observations have been made in the Arctic Ocean. The Department of Energy's (DOE) Atmospheric Research Program (ARM) maintains a station at Barrow, Alaska on the Arctic coast which contains all of the meteorological and radiation observations made at the SHEBA Ship. A few other weather stations are maintained on the northern coasts of Siberia, Alaska, and Canada collecting basic weather data for the World Meteorological Organization (WMO) network. But the daily information on meteorological conditions over the Arctic Ocean comes from extrapolation of the coastal stations by numerical weather forecasting models.

The first uses of the FIRE/ACE data set will be for development of models to describe the relationship of radiative transfer through the atmosphere to cloud and aerosol concentrations at the location of the ship and to describe how the radiative and cloud processes relate to the meteorological conditions at the SHEBA Ship. These studies will naturally need to assume that the FIRE/ACE data are typical of the Arctic Ocean. This paper examines the similarities and differences of the FIRE/ACE period to other studies made of the Arctic in other years.

More advanced uses of FIRE/ACE data set will be made by global modelers. To understand climate and predict its change, the entire earth has to be considered as one system. The global modelers need to seamlessly model clouds and radiative processes from the tropics through mid-latitude storm belts, into the Arctic Ocean. The similarities and differences of Arctic weather systems to lower latitudes is necessary knowledge for the development of global climate models.

To compare the meteorological conditions encountered during FIRE/ACE with other years and latitudes, the global analysis of the National Ocean and Atmospheric Administration's (NOAA) National Center for Environmental Prediction (NCEP) is used. This analysis is made twice per day and is the starting point for weather prediction models run by NOAA NCEP. A similar analysis also is made by the European Center for Medium Range Forecasting (ECMWF). The ECMWF gave the FIRE/ACE program its analysis only for the location of the SHEBA Ship – one point in the Arctic Ocean. This paper discusses weather systems, storm tracks and movement, which requires analyses over most of the western Arctic Ocean. ECMWF made only part of their spatial analyses fields available and these fields were similar to the NOAA NCEP analysis. Also, past studies of Arctic Ocean meteorology have used the NOAA NCEP analysis, so for consistency, this paper uses only the NOAA NCEP analysis.

Former studies of the Arctic Ocean meteorology discussed the frequencies of cyclones using the NOAA NCEP analyses,

Serreze et al. (1993) and Key and Chan (1999). The frequency and movement of cyclonic and anticyclonic weather systems during FIRE/ACE will be discussed in Section 2 and compared to the previous studies. Weather and temperature records will be discussed in Section 3. A comparison of the SHEBA Ship observations to the NCEP analysis also is given in Section 4. The SHEBA Ship observation was available for the NCEP analysis. However, the analysis did differ from the Ship's observation which gives an indication of the quality of the NCEP analysis.

Air parcel trajectories have also been studied in the past by Harris and Kahl (1994), Jaffe et al. (1995), and Bodhaine and Dutton (1995) to explain the sources of air pollution in the Arctic. In Section 5 air parcel trajectories for the FIRE/ACE aircraft flights are discussed because cloud and ice condensation nuclei (CCN) were measured in the FIRE/ACE flights. The sources of these nuclei will be compared to the previous studies of Arctic nuclei sources.

Cloud forms also have been studied by Curry et al. (1996) and Schweiger et al. (1999) for understanding the radiative heat balance of the Arctic Ocean. FIRE/ACE cloud data are compared to the previous studies in Section 6.

2. Pressure systems affecting the SHEBA Ship

Most cyclones (lows) enter the Arctic Ocean in the Norwegian Sea (see Figure 1) according to Serreze et al. (1993). However, Serreze et al. (1993) notes that the Beaufort and Chukchi Seas opposite the pole in the western Arctic (north of Alaska) experience < 1/3 of the cyclone activity of the Norwegian Sea. Serreze et al. (1993) counted 51-53 cyclones per month north of 65° latitude in April through July covering the whole polar cap . The hemisphere north of 65° latitude includes large land masses in Greenland, Canada, one half of Alaska, and part of Europe and Siberia which will not be discussed here. The northern coast of Alaska is about 70° north latitude. The Siberia coast varies between 70° and 75° north, while the Canadian Islands and Greenland extend up to 82° north. Of the 50 cyclones per month north of 65° latitude reported by Serreze et al. (1993), we would expect five or less per month in the Chukchi and Beaufort Seas near the SHEBA Ship Ice Camp. They are expected to come primarily from the south, the Bering Straight and the Siberian Coast.

The SHEBA Ship was in the northern Chukchi Sea (Figure 1) at 76° north and 164° west at the start of FIRE/ACE in April and moved slightly north and east to 78.4° north and 162.1° west by the end of the period on 29 July 1998. The barometric record (Figure 2) reflects the passage of the cyclones and the anticyclones (high pressure systems) showing large changes over several days. The cyclone and anticyclone activity for each month is summarized as follows:

2.a. *April*

In April 1998 four cyclones (lows) passed the Ship (Figure 3). The first came from the Bering Straight to the south. It entered the Chukchi Sea on 6 April and quickly moved northward leaving the SHEBA Ship on 9 April. A small barometric decrease for part of 8 April indicated a possible passage of a weak cold front. This front was not visible in the cloud patterns seen on the satellite images. The next event was the passage of an anticyclone (high) north of the ship on 15 April.

A cyclone (low) came from the southern Chukchi Sea on 15 April and remained south of the SHEBA Ship. A second weak cyclone also came from the south on 19 April passing east of the Ship. This cyclone crossed Alaska moving into the Arctic Ocean at Barrow, AK.

An anticyclone (high) passed SHEBA Ship to the north on 25 April moving on a westward track. This anticyclone passed closer to the Ship than the previous one resulting in a greater barometric pressure recording.

2.b. ***May***

The pressure systems in May lingered near the ship for longer periods than the previous month. 1 May is Julian day 121 and 31 May is Julian day 151 in Figure 2. The first cyclone passed north of SHEBA Ship on 3 May. It is shown in the April panel of Figure 3 because it was first seen in the western Arctic on 29 April. A front crossed the Ship on 3 May indicated by the dip in barometric pressure (Figure 2). The anticyclone (high) that followed was very broad and weak. It moved slowly from the southwest (the lower Chukchi Sea) moving northeast.

A second cyclone (low) passed SHEBA Ship on 12 May. This cyclone (low) came from the south (lower Chukchi Sea) moving northeastward. It was followed by a large anticyclone (high) that came from the northwest and stalled over the Ship for six days. As this anticyclone moved east, the winds shifted to a southerly direction and the temperatures rose above the freezing point for the first time on 28 May.

The last event of the month was a small cyclone that came from the Siberian Coast to the south. It moved north passing the Ship to the west on 30 May. Figure 3 also shows two other cyclones (lows) that moved north from Alaska in the eastern Beaufort Sea which were far from the Ship having no effect on it. An anticyclone (high) also moved across the eastern Beaufort Sea in the same northward direction on 31 May. It didn't affect the Ship until it intensified on 4 June.

2.c. ***June***

The anticyclone (high) that came from Alaska on 30 May strongly affected the Ship on 4 June as it traveled northeast (shown in the May panel of Fig. 4). It was followed by an eastward traveling cyclone that came from the Laptev Sea in the west, passing SHEBA Ship to the north. The passage of a front from this cyclone is indicated on the barometric record on 7 June.

Most of June was dominated by a large anticyclone (high) that first appeared in the Chukchi Sea to the south on 10 June, moved east into the Beaufort Sea, turned north in the Beaufort Sea on 13 June, and then turned west on 22 June moving past SHEBA Ship's north side. While the anticyclone (high) was far to the east in the Beaufort Sea, a cyclone moved past the Ship on 21 June on a track from the Siberian Sea, heading southeast into the Chukchi Sea. The SHEBA Ship felt the effects of the large anticyclone (high) a second time on 24 June when it was on its north side. Another large cyclone (low) on 27 June, came out from the south across the eastern tip of Siberia and headed north toward the pole passing SHEBA Ship's west side on 29 June.

2.d. ***July***

July had even less cyclonic activity than June. A cyclone (low) came past the Ship from Siberia heading north on 4 July following nearly the same track as the cyclone that passed on 29 June. It was followed by a small anticyclone (high) coming from nearly the same location in Siberia, but it headed northeast and quickly dissipated west of the Ship without leaving a pressure maximum on the barometric record (Figure 2b).

The strongest anticyclone (high) came from Siberia entering the Chukchi Sea on 7 July and moving eastward into the Beaufort Sea. It changed direction on 12 July, moving north and then merging with another strong anticyclone on 13 July that came across the Arctic north of the Ship. The large anticyclone dominated the Beaufort Sea for most of the month moving around the northern part of the Beaufort Sea close to Canada. Some cyclones (lows) moved north past the Ship coming from the Laptev Sea in western Siberia.

The mean direction of cyclone (low) motion in the summer was from southwest to northeast according to Serreze et al. (1993). Many cyclones in April through May 1998 had this general direction. However, there were several westward moving cyclones as well. The mean sea level pressure pattern in Serreze et al. (1993) also shows a high (anticyclone) in the eastern Beaufort Sea. A high (anticyclone) was in this area for most of June and July

1998. But the anticyclones had considerable movement in location from day-to-day causing complicated records of barometric pressure and winds.

3. Surface temperature and weather

SHEBA Ship measured temperatures from -7° to -28° C in April (see Figure 5). During May temperatures steadily rose with the first thawing reported on 28 May (Julian Day 148). During June the temperatures oscillated from –4° to +1° C. In July the temperature range was even smaller from –2° to +2° C. Dew points were generally close to the temperatures resulting in high humidities.

Low visibility (≤2 nm) was reported 16% of the time in April 1998 (See Table 1). With the increasing fog in the summer months, low visibility reports increased to 43% in July 1998. Snow (S), blowing snow (BS), and ice crystals (IC) were reported 15% of the time in April (Table 1) increasing to 26% of the time in May. June and July 1998 had few snow reports (5% each month). Snow was not correlated with low visibility in May when less than one half of the snow reports (12% of all reports) had both snow and low visibility (Table 1). Fog reports were rare in April and May, 6-7%, but very common in June and July 24-26%. Drizzle and rain also were occasionally reported in May-July, 3-4% of the time.

4. The accuracy of the NCEP analysis

NCEP analysis and forecasts were compared to the SHEBA Ship observations reported to the WMO for May through July 1998. Four measurements were statistically compared, the surface temperature, dew point, wind speed, and pressure. The comparisons were made at 00 UTC each day by extracting values at the location of SHEBA Ship from the NCEP surface analysis and forecast fields. The Final Analysis product of NCEP along with the forecasted fields from the Medium Range Forecast model (MRF) were used. No products from the Aviation run or limited area models were compared. The current position in the WMO report from the SHEBA Ship was updated daily for each comparison. Summaries of the mean biases of each variable and the root mean squared error are shown in Figure 5 and Tables 2 and 3.

The Ship's WMO observations were available to NCEP so the comparison to the daily analysis is not statistically independent. However, the NCEP analysis should not be expected to have the same values reported by the SHEBA Ship because the analysis has to consider consistency between dynamic and thermodynamic fields and maintain consistency of these fields in time. A radical data value could generate fictitious waves in the model's fields if inserted directly into the analysis. The analysis system blends the observation with the forecast generated by the previous run of the MRF model. Any observation that deviates radically from the forecast values, is discarded by the analysis system suspecting and error in the observation. NCEP did not keep a record of the use and/or rejection of the SHEBA Ship data. These data entered into the analysis system with thousands of other WMO data. Because of the complicated analysis system, a comparison between the Ship's data and the analysis at the Ship's location was made to show how well the analysis reflected the data.

The NCEP analysis had mean biases of +0.3° C in temperature, -0.6° C in dew point, +0.4 m/s in wind speed, and +1.9 hPa in sea level pressure over the April through July 1998 period (See Table 1). However, there were monthly changes in the biases (see Table 3). The NCEP analysis was

biased warm in April and May by 1.0° to 1.5° C. In June the bias reduced to 0.2° while in July it changed sign to –1.0°. The warm biases occurred when the temperatures were cold - April averaged –15.6° C and May averaged –8.3° C. The negative bias occurred when the temperature was close to the freezing point - June averaged –0.3° C and July averaged +0.6° C.

A t-test for significance of these biases was made (Panofsky and Brier, 1968; and Dixon and Massey, 1969) using the null hypothesis that the NCEP analyses and ship observations were from the same population and thus the mean bias should have been zero. Daily biases were calculated from the paired NCEP analysis values and observations at 00:00 UT.

$$B(d) = T(d)_{NCEP} - T(d)_{ShipObs} \quad (1)$$

The t-test estimated the probability of (non-zero) monthly averaged biases occurring by random chance (in a two tailed distribution). It is based on the standard deviation of the daily biases and the number of days used in the monthly averages. Standard deviations (STD) were calculated from the daily biases by:

$$STD = \frac{\Sigma \left[B(d) - \overline{B} \right]^2}{(n-1)} \quad (2)$$

The number of paired daily observations (n) used in each month ranged from 22 to 30. The monthly averaged biases were considered to be significantly large where the t-test found the probability of it occurring by chance to be <1%. These values are italicized in Tables 2 and 3.

The t-tests indicate that NCEP analysis has significant biases in May and July but not in April and June. The t-test was also applied to the dew point, wind speed, and sea level pressure data (see Tables 2 and 3). Dew point biases were small and insignificant in April, May, and June, but in July they were significantly biased cold by -1.4° C. Wind speed biases also were small in April through June, but significantly biased high by 1.3 m/s in July. Sea level pressures were significantly biased negative in all four months by –1.2 to 2.8 hPa.

Wind directions are also shown in Figure 5. Bias statistics were not calculated because wind directions have little meaning when speeds are low. The time plot (Fig. 5) shows general agreement of the NCEP analysis with the SHEBA Ship reports on most days.

The forecast values of temperature, dew point, wind speed, and sea level pressure from NCEP Medium Range Forecast (MRF) model also were compared to the SHEBA ship observations (Table 2). The same t-test for significance of the differences between the forecast values and observations was applied. The forecasts of all four parameters had significant biases over all three forecast intervals. Temperatures were biased warm from 1.5° in the 24 hour forecast increasing to 1.8° in the 72 hour forecast. Dew points also were biased warm by 1.5° to 1.7°. Wind speeds were biased high from 0.7 to 1.3 m/s and sea level pressures were biased low by 1.8 to 2.4 hPa.

The objective of the FIRE/ACE forecast was prediction of cloud occurrences and the type of clouds for planning aircraft flights. This task is very difficult because of the lack of good cloud products from any of the forecast models. Cloud predictions were based on the pressure patterns using methods identical to those used in lower latitude FIRE experiments in the past. A quantitative score was not kept of the cloud forecasts, but the qualitative estimate was that clouds were harder to predict in the Arctic Ocean than other areas because of the preponderance of many small cyclones and anticyclones that daily changed form, intensity, and direction of movement. The quality of guidance of the NCEP MRF and ECMWF models was surprisingly good considering the lack of data at high latitudes and the absence of upper air data in the Arctic Ocean, except for the SHEBA Ship sounding.

5. Air Trajectories

Back trajectories of air were computed from the wind analyses of the NCEP Final Analysis available in 12 hour intervals. Air parcel histories were calculated by interpolating the wind fields analyzed by NCEP on constant pressure surfaces, to isentropic surfaces, and then calculating displacements backward from the ship in one hour increments. The back trajectory calculations were limited to 6 days. Summaries for individual FIRE/ACE flights can be found at http://www.ssec.wisc.edu/~donw/sheba which is referenced by the FIRE/ACE web page.

5.a. *April*

Most surface trajectories come from the east (Figure 6) because of the cyclones (lows) in the Bering Straight, Chukchi Sea and northern Alaska. This occurred on twelve of the fifteen days analyzed (80%). Only three trajectories traced back to the north when a surface high was northwest of SHEBA Ship. Most of the surface air thus came from the Beaufort Sea and Arctic Canadian Islands east of the Ship. Only three surface trajectories indicate air coming from Europe across the North Sea and from western Russia.

The higher altitude trajectories, (see Figure 7) trace back to the south or southwest reflecting the dominance of a southerly upper air flow pattern. Ten of the 15 trajectories came from the North Pacific Ocean across Alaska and one came north through the Bering Straight. In general, the upper air trajectories could be traced back to the North Pacific Ocean on 73% of the days studied in April 1998. This air usually was ascending as it flowed north from the Pacific to the Arctic Ocean (see Figure 8) which contributed to frequent cloud cover. Only two of the 3 km altitude trajectories traced back to Europe.

5.b. *May*

Surface trajectories (Figure 9) show the dominance of the anticyclone (high) in the Beaufort Sea to the east. Ten of the 16 trajectories (63%) have anticyclonic curvature in the Beaufort Sea to the east indicating the air had been in the Beaufort Sea for at least six days. A group of four low level trajectories traced back to the south, the Chukchi Sea and eastern Siberia, and two others traced southwest to the Siberian Sea. These six trajectories account for 37% of the days studied in May. They occurred when the cyclones came north past the SHEBA Ship. None of the May trajectories traced back to Europe.

Upper air trajectories (Figure 10) also appear to have two modes. Nine trajectories (56%) are local anticyclonic gyres north of SHEBA Ship indicating the air came from an anticyclone locally in the Arctic (over the last six days). Six trajectories (38%) show air coming from the North Pacific Ocean across Alaska and the Bering Straight and one trajectory traced back to Siberia.

5.c. *June*

Surface and upper air trajectories (Figures 11 and 12) show a variety of directions. When the large anticyclone was present, seven surface trajectories (44%) traced back to the east in the Beaufort Sea in an anticyclonic gyre. Four of those trajectories were close to the Alaskan coast while three were in the northern Beaufort Sea. Three other trajectories (19%) traced south to the Pacific and Bering Straight. Two traced to Siberia (12%). Two traced west to the Laptev Sea and Russia (12%) and two others traced northeast back to the North Sea by Europe (12%).

Higher altitude trajectories (Fig. 12) had slightly different trajectories with five coming across the pole (31%). However, two of the polar trajectories were large gyres that trace back to the central Arctic Ocean in six days and two trace to Greenland. Only one leads back to Russia and eastern Europe. Two others traced back through the Siberian sea to eastern Russia (12%). Six traced south to the North Pacific Ocean.

5.d. *July*

The surface trajectories (Fig. 13) reflect the large anticyclone in the Beaufort Sea to the east with anticyclonic gyres. Five

of eight surface trajectories have anticyclonic obits in the Beaufort Sea (62%). One traced south to the North Pacific (12%) while two reached across the Arctic back to Europe (25%).

The higher level trajectories (Fig. 14) traced around the high for the later flights from 28-30 July remaining in the Arctic. Two traced east to the Canadian Arctic Islands by two gyres in opposite directions. Two traced south through Alaska, one into Siberia, while one traced northwest through Russia to Europe.

In general these trajectories show 25-40% of the air in each month coming from the North Pacific Ocean over Alaska, the Bering Straight, and eastern Siberia. Many of the surface trajectories also traced east into the Beaufort Sea or were confined in gyres near the SHEBA Ship. Very few traced back to Europe or Russia.

These trajectories compare favorably with the studies of Barrow made by Miller (1981) and Harris and Kahl (1994) that show a variety of air sources, mostly from the south. However, studies by Rahn and Lowenthal (1986) and Shaw (1982) have indicated the possibility of European sources of air pollution in northern Alaska from chemical tracers. The FIRE/ACE flights sampled very few cases where air came from Europe across the Arctic Ocean. Most air sampled in the FIRE/ACE flights had North Pacific and Alaskan origin, or resided in the Beaufort Sea locally for at least six days prior to reaching the SHEBA Ship.

6. Cloud Frequency

The cloud cover reported to the WMO Synoptic system by the SHEBA Ship varied between 69 and 86% (Table 2). This is the monthly average of the WMO reports (in octas) filed every six hours. April averaged 69% cloud cover, steadily increasing to 86% in July 1998.

Satellite estimates of cloud frequency were made by the Wisconsin HIRS analysis (Wylie and Menzel, 1999) using three polar orbiting satellites which is an on-going global cloud climatology. All HIRS data were averaged from 75° to 79° north and 160° to 166° west (Table 4), the region around the Ship. This analysis reported nearly 100% cloud cover for all four months of FIRE/ACE. The geographical distribution for July 1998 was shown in Figure 1.

The Wisconsin HIRS analysis appears to have excessively large cloud frequencies. Part of the problem is that it is dependent on the NCEP analysis of surface temperature which averaged 1.3 C above the temperatures reported by the Ship in the first two months. The NCEP surface temperature bias in April and May probably caused the Wisconsin analysis to classify HIRS fields of view (FOV) with broken cloud cover, as totally cloudy. Partial FOV coverage cannot be determined from the HIRS data at low altitudes. Broken cloud fields were common because 95-99% of the SHEBA Ship reports contained some cloud coverage (Table 4).

Data from other years analyzed by Schweiger et al. (1999) and Curry et al. (1996) found cloud cover averaging 60-85% in the Arctic. The lower values came from cloud cover calculations that ignored fog and other visibility obstructions because the observers could not see if clouds were above the surface obstructions. Schweiger et al. (1999) also reported cloud frequencies of 75-80% in the summer of 1990 using the TOVS Pathfinder analysis of HIRS data. The Wisconsin Analysis of HIRS data appears to have overestimated the cloud cover of the Arctic Ocean compared to the studies of Curry et al. (1996) and Schweiger et al. (1999) because the Wisconsin Analysis does not distinguish small clear parts of low level cloud fields. Fog and haze also are included in the count of low clouds.

The Wisconsin HIRS analysis was designed for identifying high clouds, especially thin cirrus which are semitransparent to terrestrial radiation (Wylie et al., 1994). It surpasses the

International Satellite Cloud Climatology Project (ISCCP) in detection of semitransparent cirrus clouds (Jin et al., 1995; Wylie and Menzel, 1999). The "High Clouds" in Table 4 include all HIRS reports above 400 hPa pressure altitude which is about 7 km. Middle clouds are from 700 to 400 hPa which is 3-7 km. High clouds were rare, occurring only 6-10% of the time in April-June. In July 1998 they increase to 26% of the time. July 1998 had more high clouds than the 10 year average, whereas the other months where close to the 10 year mean. Middle level clouds, a 39% occurrence in both April and May 1998, were less frequent than the 10 year mean of 57-61% in the spring months. However, in June and July, middle cloud frequencies of 40-55% were closer to the 10 year mean of 56-59%. The middle and high level clouds were an obstacle to the objectives of FIRE/ACE which wanted to focus on the radiative properties of the ice surface and boundary layer arctic stratus clouds. The 10 year history of the Wisconsin HIRS observations indicate that middle and high clouds above 700 hPa (3 km) occur 61% of the time in this area. May –June 1998 were close to this average while July 1998 had more higher level clouds above 400 hPa (7 km) but less middle level clouds, resulting in the same combined occurrence frequency above 3 km and conforming to the 10 year mean.

7. Summary

The synoptic activity consisted of eleven cyclones (lows) passing the SHEBA Ship in April through May 1998 and approximately 10 anticyclones (highs) spreading toward the Ship in between cyclone passages. Eleven cyclones in four months is close to the number expected from the synoptic climatology of Serreze et al. (1993). The cyclones came primarily from the south and southwest as expected from the Serreze et al. (1993) climatology. However, there were four deviations from this track - three came from the northwest and one came from the northeast and moved west in April. Westerly movement of cyclones is rare in lower latitudes. In June another rare cyclone also came from the northwest, the Laptev Sea in north central Russia, and moved southeast into the lower Chukchi Sea eventually merging with a cyclone in eastern Siberia. This path also was contrary to the others that came out of Siberia, the Bering Straight, and the lower Chukchi Sea.

The anticyclones (highs) had even more erratic movements than the cyclones. In April two came from the east moving west passing the Ship to the north. In June one very large anticyclone moved around the Ship coming from the Siberian coast. It moved east into the Beaufort Sea and Alaskan coast and eventually moved north in the eastern Beaufort Sea along the Canadian Islands and then finally turned west passing north of the Ship. This anticyclone dominated the eastern Beaufort Sea for most of June. It spread westward affecting the SHEBA Ship in between passages of cyclones (lows). Anticyclonic activity dominated the Beaufort Sea southeast of the Ship in July. Movement and intensity of these cyclones was erratic with mergers and dissipation of anticyclonic centers. The daily movements of these synoptic systems (cyclones and anticyclones) are more complicated in the Arctic Ocean than their relatives in lower latitudes.

Air temperatures rose from the winter-like conditions (-15° to -20° C) in early April to the freezing/thawing point at the end of May and remained close to this point through July. This too, appears to conform to climatological norms. The NCEP analysis of surface temperature and dew point were biased warm by +1.0° to +1.5° C until the air temperature reached the freezing/thawing point in late May. In July, during the warmest period, the NCEP analysis was biased cold by –1.0° C. Dew points followed the same patterns as temperatures. However, the NCEP analysis

didn't show a significant bias until July where it was cold by –1.4° C. The NCEP surface pressure analysis was consistently biased low from the SHEBA Ship observations in all months by –1.2 to –2.8 hPa. The monthly averaged biases in the wind speed analysis were small and insignificant until July where it averaged 1.3 m/s. However, July had few high wind days – only one exceeded 10 m/s. For the four days in June and one in May with winds >10 m/s, the NCEP analysis was biased low by an average of –2.2 m/s. The wind directions of the NCEP analysis generally agreed with the Ship reports.

Air trajectories were generally from the south and southeast. Some previous studies predicted that more air masses could be traced back to Europe and Russia. These cases were few in the April-July 1998 period. If air pollution sources are found in these data, they most likely will be in eastern Siberia, Alaska, or western Canada because most of the air entering the Arctic during the four months studied came from these regions.

Clouds appeared to follow climatological norms. The SHEBA Ship was located where southerly flow is very common because of the anticyclone in the Beaufort Sea and the cyclonic activity to the west of it. The southerly flow brought moisture, forming clouds at all levels. Boundary layer Arctic stratus usually occurred under higher clouds in June and July. The Wisconsin HIRS analysis indicates higher frequencies of clouds above 400 hPa (7 km) than normally found in the month of July 1998. In the other months, cloud statistics are reasonably close to the other climatologies.

8. Acknowledgements

This work was supported by grants NAG-1-1830 and NAG-1-2196 of the National Aeronautics and Space Administration (NASA). The author also appreciated the generous support of the National Oceanographic and Atmospheric Administration (NOAA) in providing data and the Alaskan Branch of NOAA in assisting in the weather forecasting for the FIRE/ACE flights.

9. References:

Bodhaine, B. A., and E. G. Dutton, 1993: A long-term decrease in Arctic haze at Barrow, Alaska., *Geophys. Res. Letters*, **20**, 947-950.

Curry, J. A., P. V. Hobbs, M. King, D. A. Randall, P. Minnis, et al., 1999: FIRE Arctic Clouds Experiment. *Bull. Amer. Meteor.* Soc., **81**, 5-29.

Curry, J. A., W. B. Rossow, D. R. Randall, and J. L. Schramm, 1996: Overview of Arctic cloud and radiation characteristics., *J. Climate*, **9**, 1731-1764.

Dixon, W. F., and F J. Massey, 1969: *Introduction to Statistical Analysis.*, McGraw-Hill Inc., New York, NY, Lib. Congr. # 68-17180, 638 pp.

Harris, J. M., and J. D. W. Kahl, 1994: Analysis of 10-day isentropic flow patterns for Barrow, Alaska: 1985-1992., *J. Geophy. Res.*, **99, D12**, 25,845-25,855.

Jaffe, D. A., R. E. Honrath, J. A. Herring, S. M. Li, and J. D. Hahl, 1991: Measurements of nitrogen oxides at Barrow, Alaska during spring: Evidence for regional and northern hemispheric sources of pollution, *J. Geophys. Res.*, **96**, 7,395-7,405.

Jin, Y., W. B. Rossow, and D. P. Wylie, 1996: Comparison of the climatologies of high-level clouds from HIRS and ISCCP., *J. Climate*, **9**, 2850-2879.

Key, J. R., and A. C. K. Chan, 1999: Multidecadal global and regional trends in 1000 mb and 500 mb cyclone frequencies., *Geophy. Res. Letters*, **26**, 2053-2056.

Miller, J. M., 1981: A five-year climatology of five-day back trajectories from Barrow, Alaska, *Atm. Envir.*, **15**, 1401-1405.

Panofsky, H. A., and G. W. Brier, 1968: *Some Applications of Statistics to Meteorology.*, Penn. State Univ. Park Press, State College, PA, 224pp.

Rahn, K. A., and D. H. Lowenthal, 1986: Who's polluting the Arctic? Why is it so important to know? An American perspective. In Arctic Air Pollution, ed. B. Stonehouse, Cambridge Univ. Press, 85-96.

Serreze, M. C., J. E. Box, R. G. Barry, and J. E. Walsh, 1993: Characteristics of Arctic synoptic activity, 1952-1989. *Meteor. and Atm. Physics*, **51**, 147-164.

Shaw, G. E., 1982: Evidence for a Central Eurasian source area of Arctic Haze in Alaska., Nature, **299,** 815-818.

Wylie, D. P., W. P. Menzel, H. M. Woolf, and K. I. Strabala, 1994: Four years of global cirrus cloud statistics using HIRS., *J. Climate*, **7**, 1972-1986.

Wylie, D. P., and W. P. Menzel, 1999: Eight years of high cloud statistics using HIRS., *J. Climate*, **12**, 170-184.

10. Tables

Table 1: Frequency (in percent) of weather reports from the SHEBA Ship Ice Camp during the four months of FIRE/ACE flights in 1998.

Month	Number of Reports	Visibility ≤ 2 nm.	Snow, Blowing S, and Ice Crystals.	S, BS, IC, with Vis. ≤ 2 nm.	Fog	Rain or Drizzle
April	89	6%	15%	11%	7%	0
May	121	23%	26%	12%	6%	3%
June	121	35%	5%	3%	26%	3%
July	111	43%	5%	3%	24%	4%

Table 2: The daily mean bias and standard deviation of the daily bias for the NCEP analysis and forecast products at the location of the SHEBA Ship for May through July 1998. Biases passing the t-test for significance above the 1% level are high lighted.

	Analysis	Forecast 24-Hr	Forecast 48-Hr	Forecast 72 Hr
	Bias St-Dev	Bias St-Dev	Bias St-Dev	Bias St-Dev
Temperature (C)	0.3 ±1.4	***1.5*** ±1.4	***1.7*** ±1.6	***1.8*** ±1.8
Dew Point (C)	***-0.6*** ±1.6	***1.5*** ±1.7	***1.7*** ±2.1	***1.7*** ±2.2
Wind Speed (m/s)	0.4 ±2.4	***0.7*** ±2.5	***1.0*** ±2.7	***1.3*** ±3.0
Pressure (hPa)	***-1.9*** ±1.3	***-1.8*** ±2.3	***-2.4*** ±3.4	***-2.1*** ±4.7

Table 3: The daily mean bias and standard deviation of the NCEP analysis for four months in 1998. Biases passing the t-test for significance above the 1% level are high lighted.

	April		May		June		July	
	Bias	**St-Dev**	**Bias**	**St-Dev**	**Bias**	**St-Dev**	**Bias**	**St-Dev**
Temperature (C)	1.0	±3.7	***1.5***	±1.2	0.2	±1.0	***-1.0***	±0.6
Dew Point (C)	0.2	±3.3	-0.3	±2.3	-0.1	±1.0	***-1.4***	±0.7
Wind Speed (m/s)	0.2	±1.9	-0.3	±2.6	0.4	±2.3	***1.3***	±2.3
Pressure (hPa)	***-2.8***	±0.4	***-2.2***	±0.6	***-2.1***	±1.4	***-1.2***	±1.4

Table 4: Cloud frequency or cloud fractions were averaged for the four months of the FIRE ACE flights in 1998. The HIRS High cloud category includes all clouds of height < 400 hPa, Middle clouds are 400≤ <700 hPa, and Low clouds are ≥700 hPa. Middle and Low cloud categories have been adjusted for the blockage of HIRS views into the lower atmosphere by higher clouds. The 10 year average is from Wylie and Menzel (1999). The Ship data are the cloud fractions reported to the WMO synoptic network (every 6 hours).

	April		*May*		*June*		*July*	
HIRS	**1998**	**10 Yr.**	**1998**	**10 Yr.**	**1998**	**10 Yr.**	**1998**	**10 Yr.**
High Clouds	9%	10%	6%	6%	10%	7%	26%	10%
Middle Clouds	39	61	39	57	55	59	40	56
Low Clouds	98	69	98	85	97	79	96	62
Total (HIRS)	100%	92%	100%	96%	100%	94%	99%	86%
Ship								
Average Cloud Fraction	69%		78%		76%		86%	
Number of reports with some cloud	95%		95%		97%		99%	

11. List of Figures

Figure 1: The mean frequency of clouds in July 1998 measured by the Wisconsin HIRS cloud analysis. The names of general geographical sites in the Arctic Ocean also are shown.

Figure 2a: The sea level barometric pressure at the SHEBA Ice Camp. Julian Day 91 is 1 April 1998 and day 121 is 1 May 1998.

Figure 2b: Same as 2a, for June and July 1998. 1 June 1998 is Julian day 152 and 1 July is 182.

Figure 3: The tracks of cyclones (low pressure centers) in April-July 1998 manually analyzed from the NCEP Final Analysis. Starting and ending dates are shown along with the central pressure on those dates.

Figure 4: The tracks of anticyclones (high pressure centers) in April-July 1998 from the NCEP Final Analysis sea level pressure field. Starting and ending dates along with central pressures are numerically shown.

Figure 5: The SHEBA Ship daily synoptic reports (solid line) and the bias of the NCEP analysis from the reports (dashed line). For Pressure and Wind Direction, the dash line represents the NCEP analysis value not the bias. 1 April 1998 is Julian Day 91, 1 May is day 121, 1 June is day 152, and 1 July is day 182.

Figure 6: Back trajectories for air reaching the SHEBA Ship Ice Camp during April of the FIRE ACE flights. Numbers indicate the air history back to 6 days.

Figure 7: Back trajectories in April which reach the SHEBA Ship Ice Camp at 3 km altitude.

Figure 8: Latitudinal cross section of April trajectories which reached the SHEBA Ship Ice Camp at 3 and 6 km altitude.

Figure 9: May surface trajectories to the SHEBA Ship Ice Camp.

Figure 10: May trajectories reaching the SHEBA Ship Ice Camp in May at 3 km altitude.

Figure 11: June trajectories reaching the SHEBA Ship Ice Camp at the surface.

Figure 12: June trajectories reaching the SHEBA Ship Ice Camp at 3 km altitude.

Figure 13: July surface trajectories to the SHEBA Ship Ice Camp.

Figure 14: July trajectories reaching the SHEBA Ship Ice Camp at 3 km altitude.

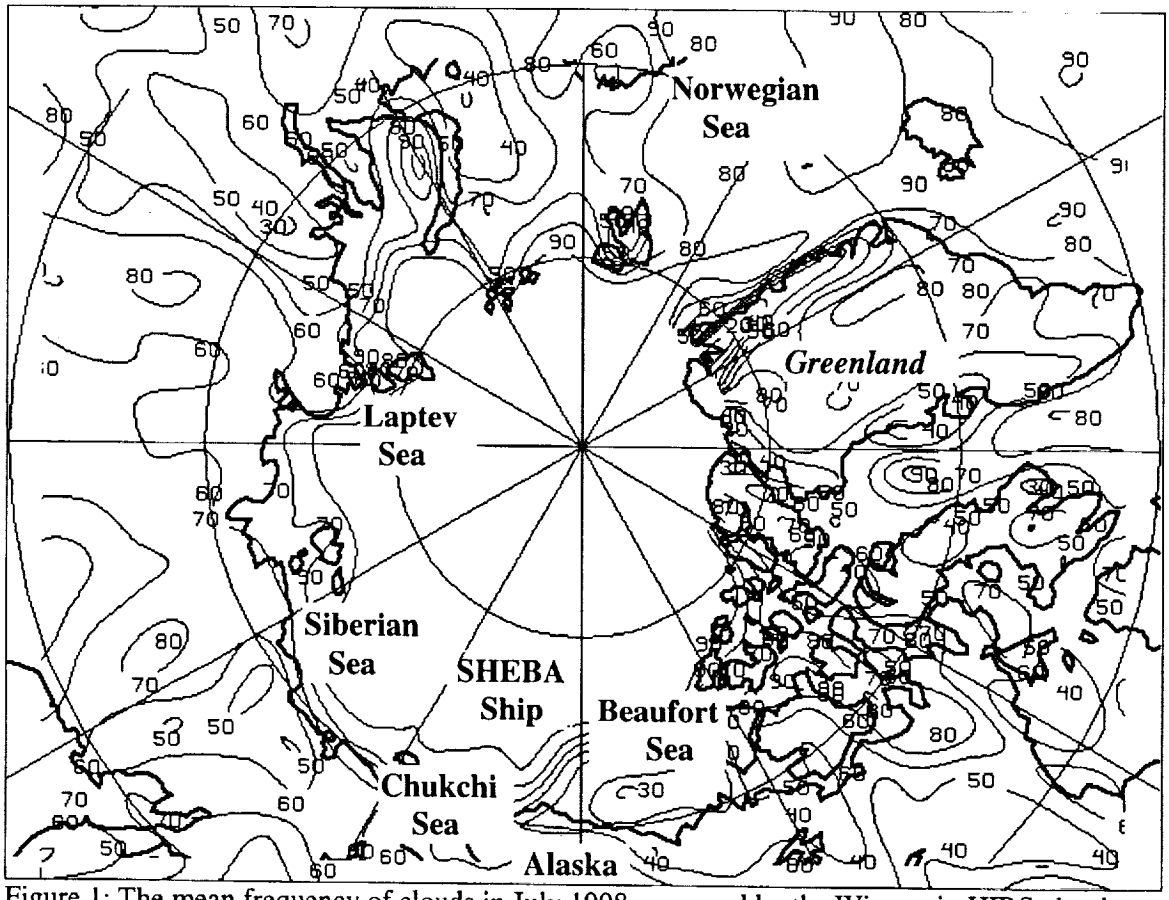

Figure 1: The mean frequency of clouds in July 1998 measured by the Wisconsin HIRS cloud analysis. The names of general geographical sites in the Arctic Ocean also are shown.

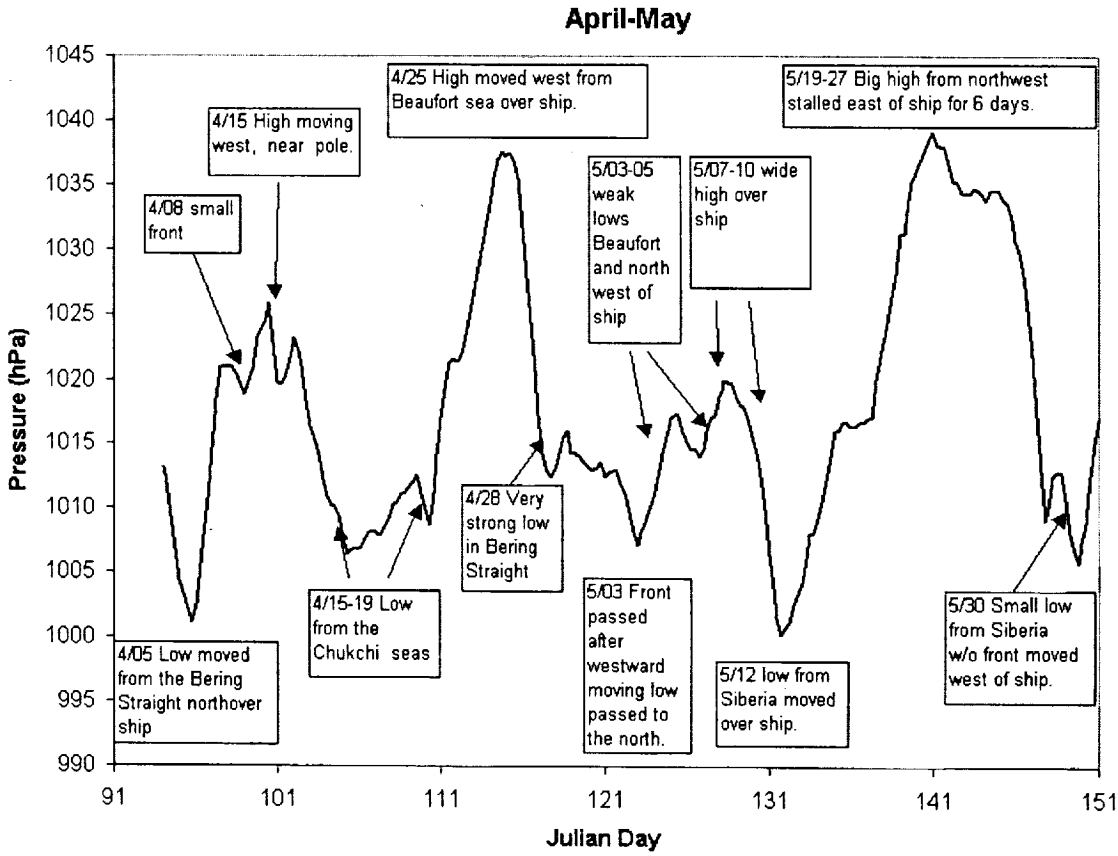

Figure 2a: The sea level barometric pressure at the SHEBA Ice Camp. Julian Day 91 is 1 April 1998 and day 121 is 1 May 1998.

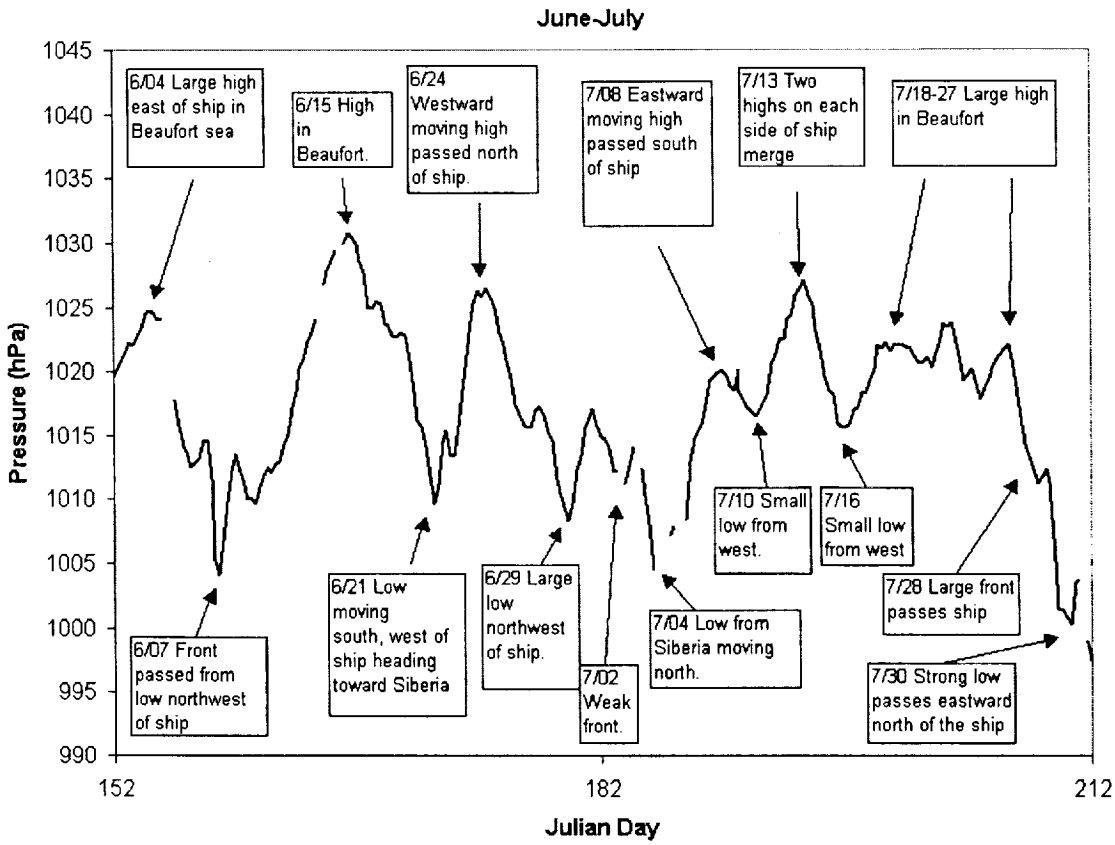

Figure 2b: Same as 2a, for June and July 1998. 1 June 1998 is Julian day 152 and 1 July is 182.

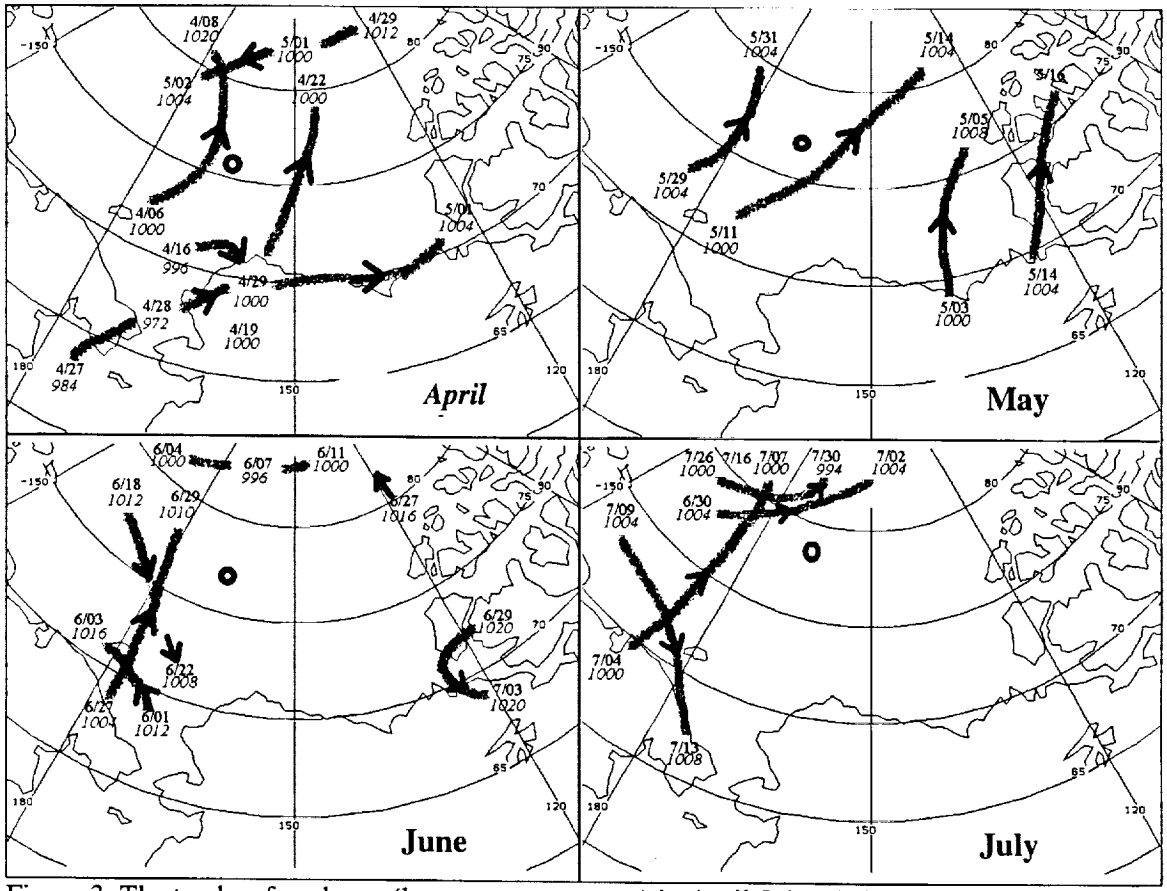

Figure 3: The tracks of cyclones (low pressure centers) in April-July 1998 manually analyzed from the NCEP Final Analysis. Starting and ending dates are shown along with the central pressure on those dates.

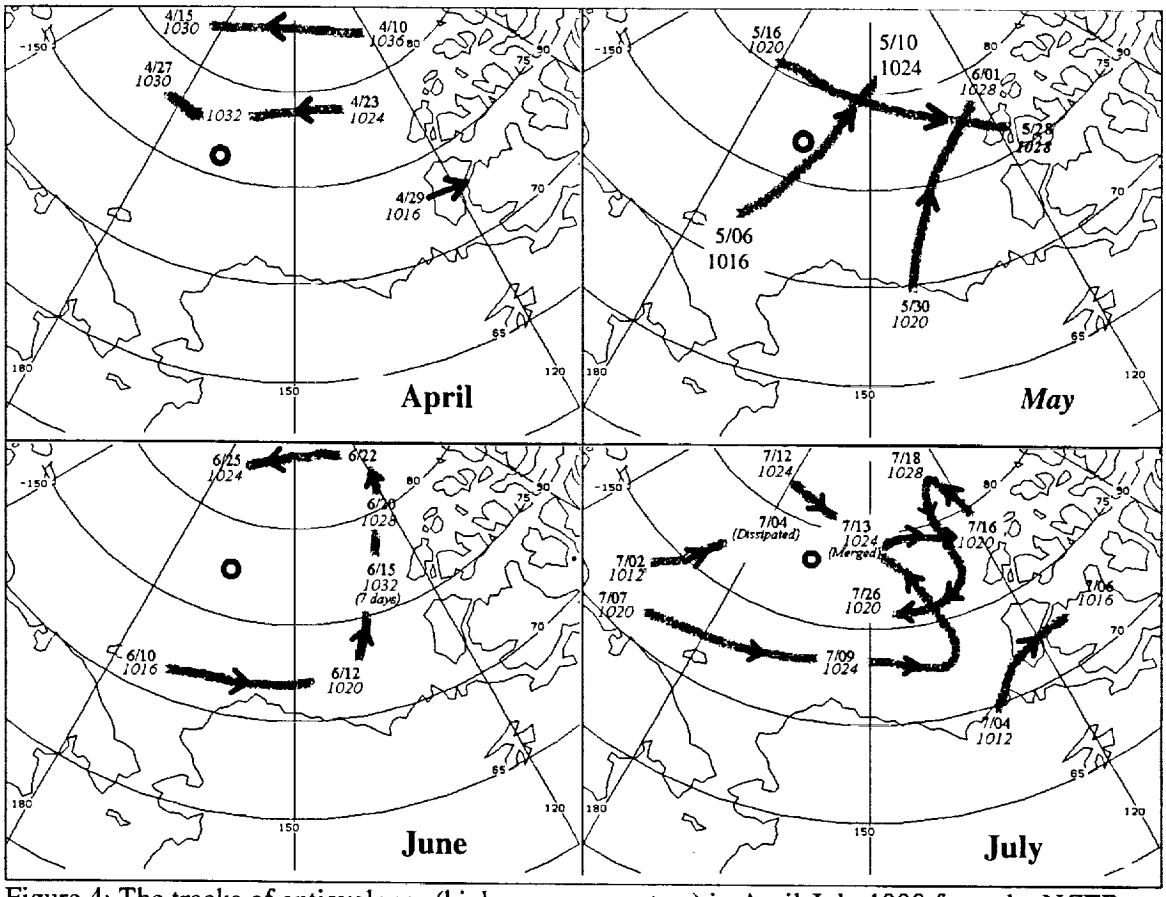

Figure 4: The tracks of anticyclones (high pressure centers) in April-July 1998 from the NCEP Final Analysis sea level pressure field. Starting and ending dates along with central pressures are numerically shown.

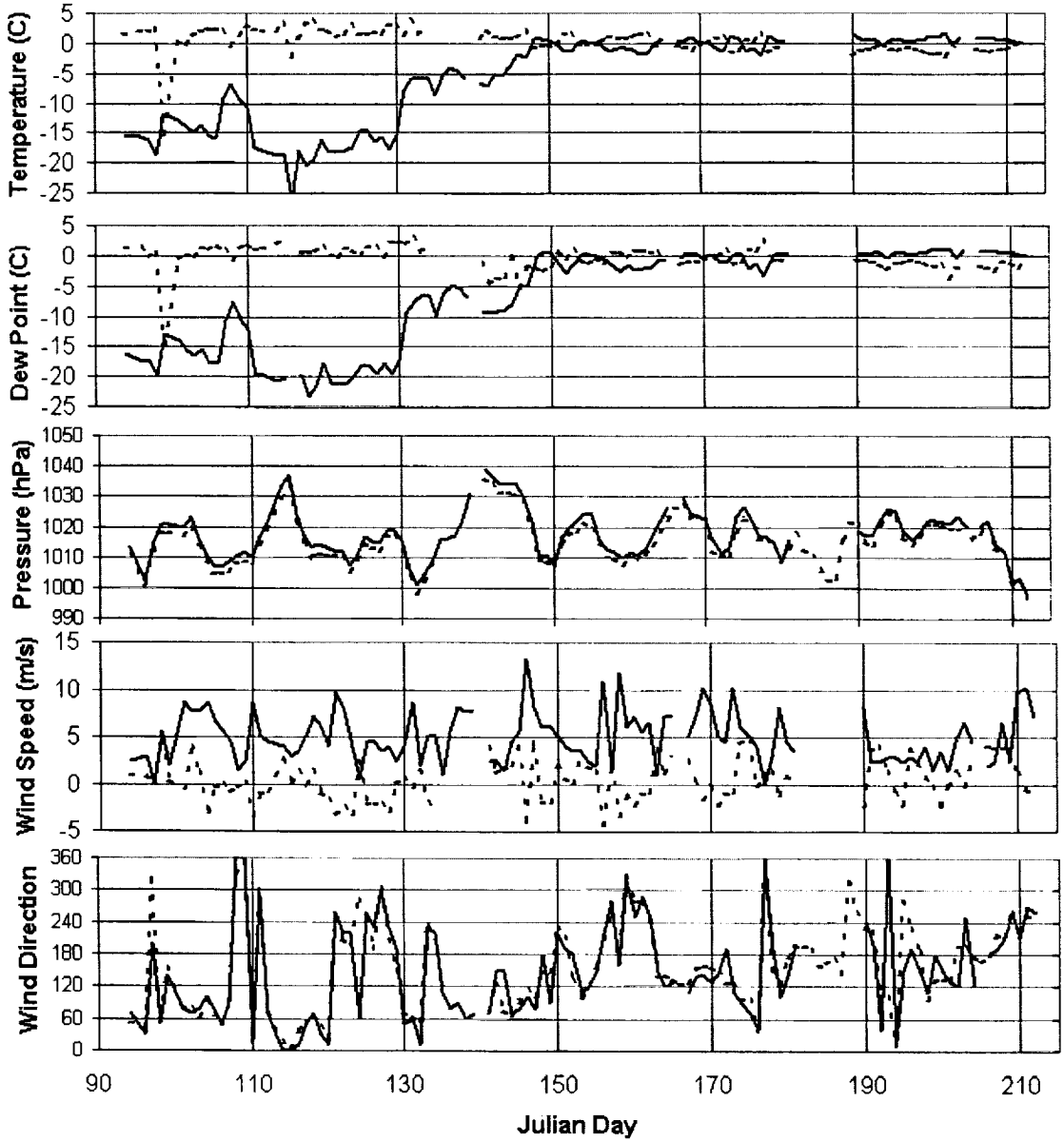

Figure 5: The SHEBA Ship daily synoptic reports (solid line) and the bias of the NCEP analysis from the reports (dashed line). For Pressure and Wind Direction, the dash line represents the NCEP analysis value not the bias. 1 April 1998 is Julian Day 91, 1 May is day 121, 1 June is day 152, and 1 July is day 182.

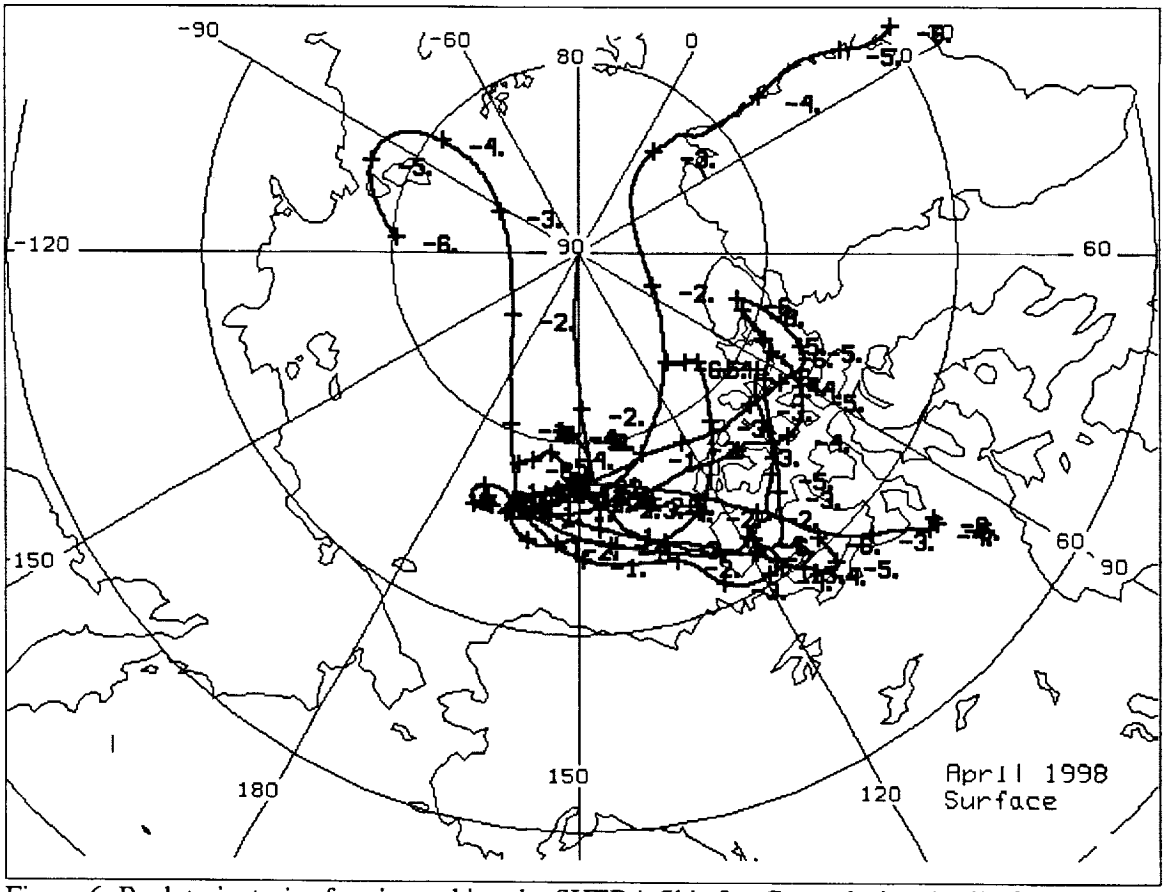

Figure 6: Back trajectories for air reaching the SHEBA Ship Ice Camp during April of the FIRE ACE flights. Numbers indicate the air history back to 6 days.

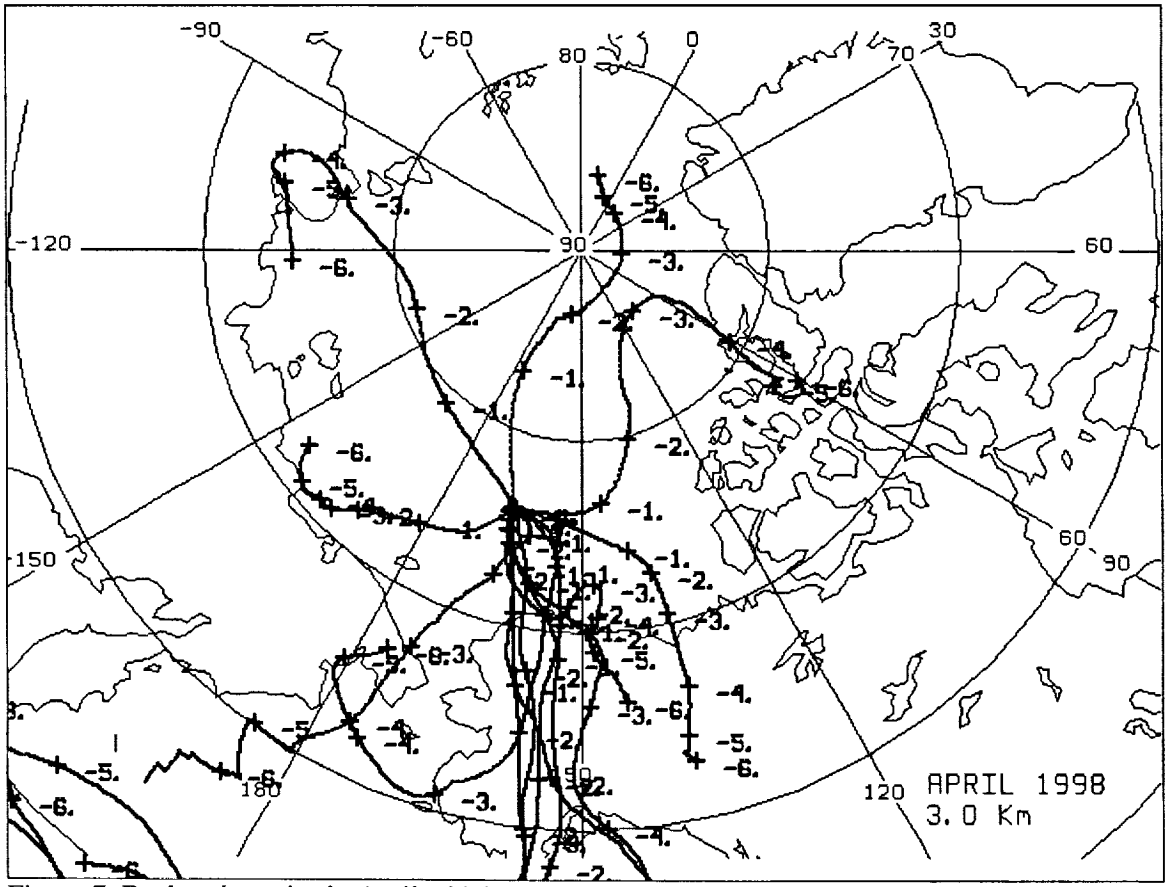

Figure 7: Back trajectories in April which reach the SHEBA Ship Ice Camp at 3 km altitude.

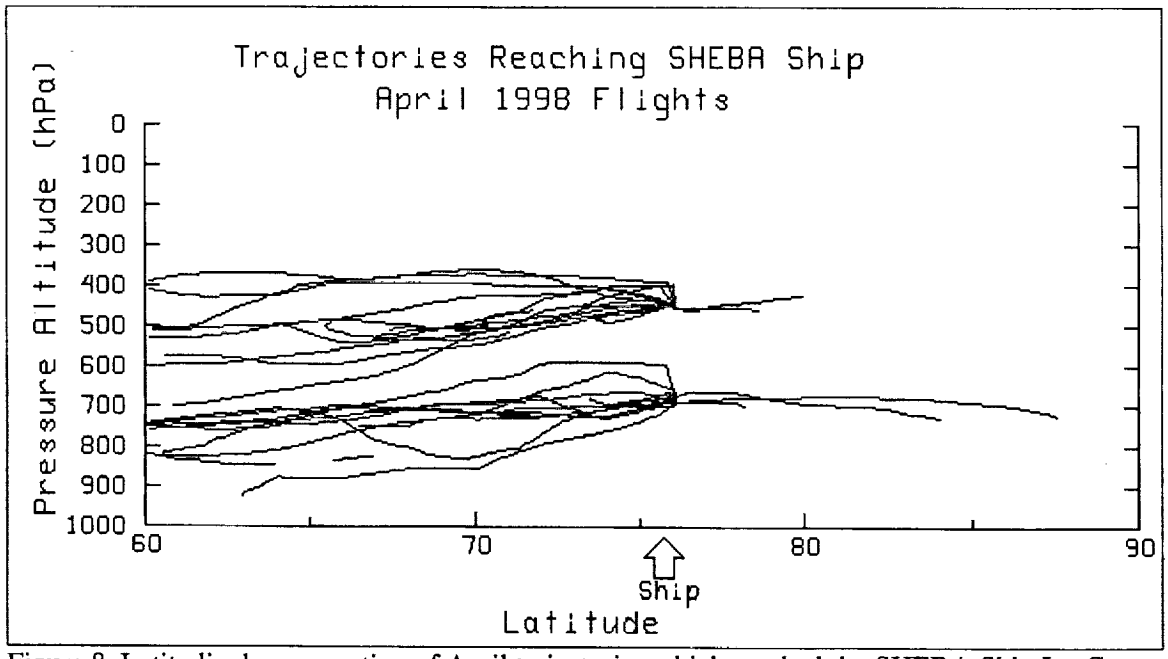

Figure 8: Latitudinal cross section of April trajectories which reached the SHEBA Ship Ice Camp at 3 and 6 km altitude.

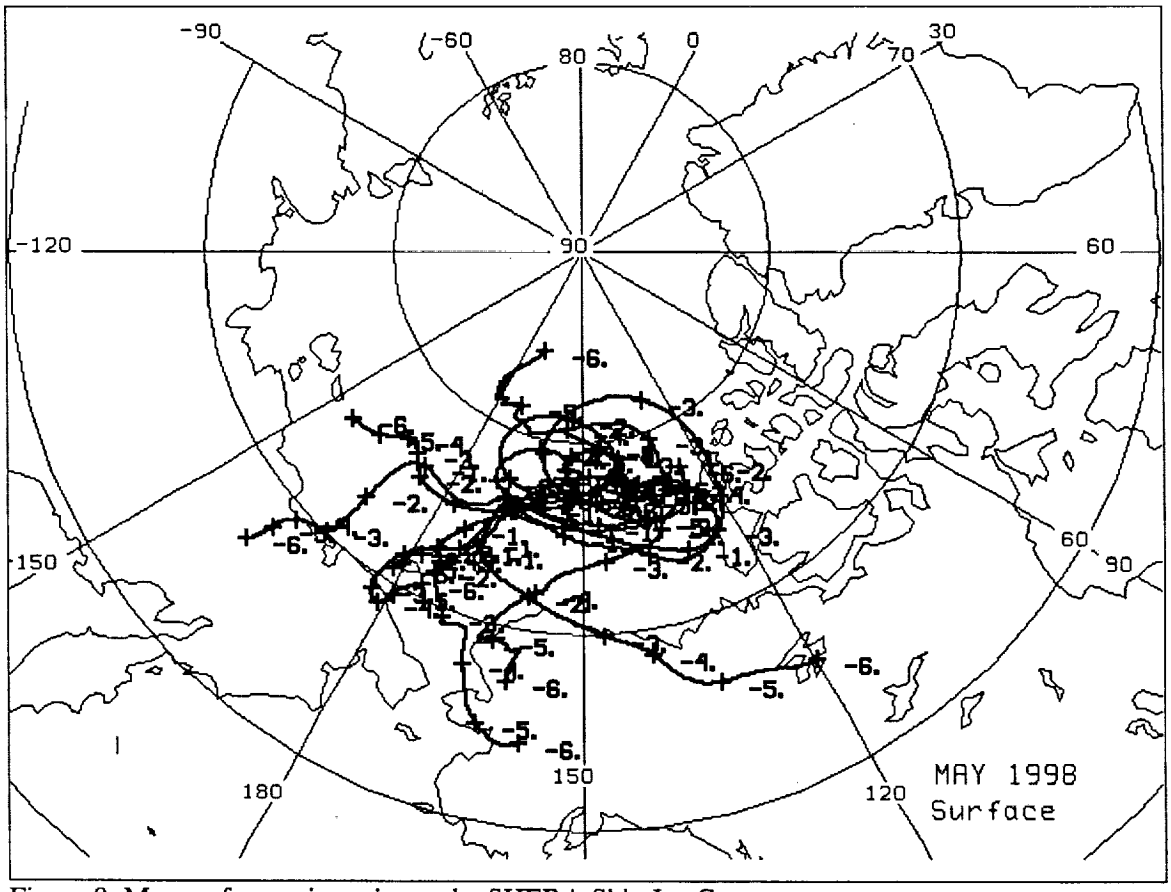

Figure 9: May surface trajectories to the SHEBA Ship Ice Camp.

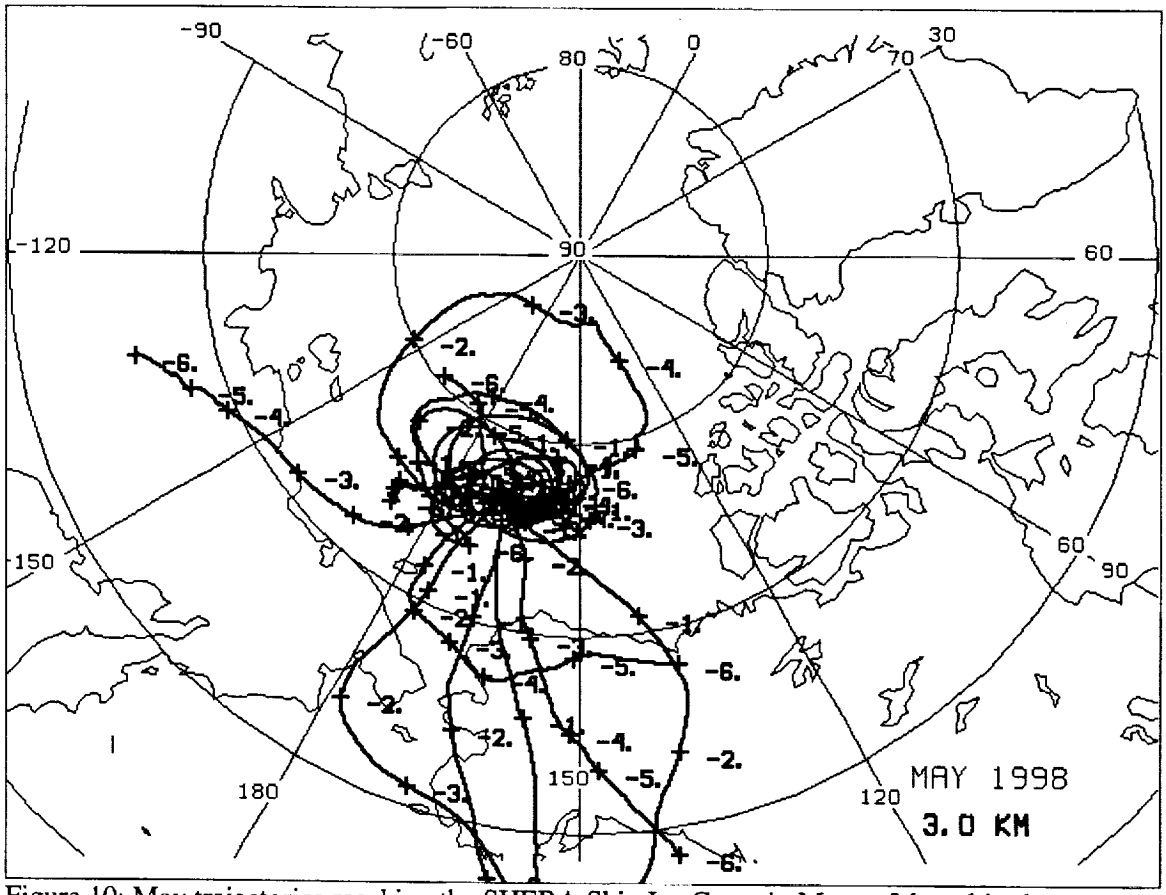

Figure 10: May trajectories reaching the SHEBA Ship Ice Camp in May at 3 km altitude.

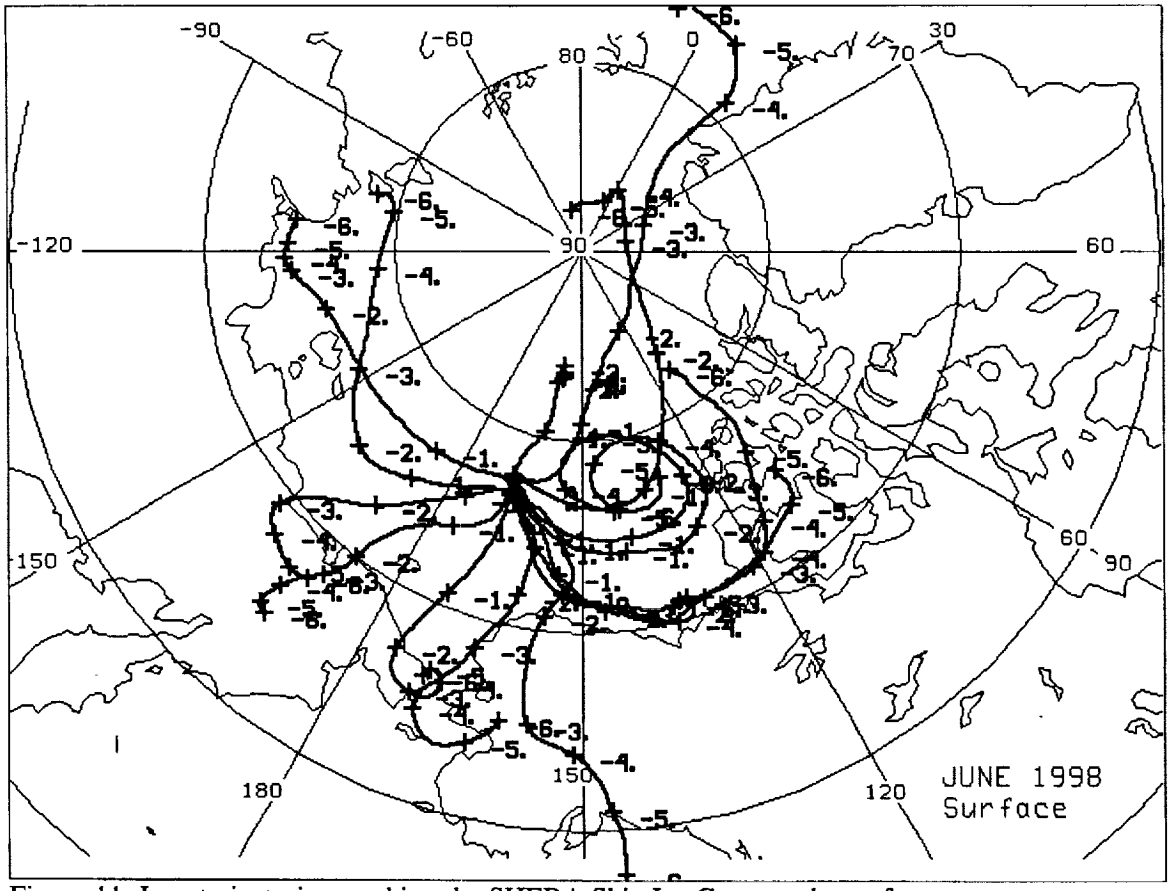

Figure 11: June trajectories reaching the SHEBA Ship Ice Camp at the surface.

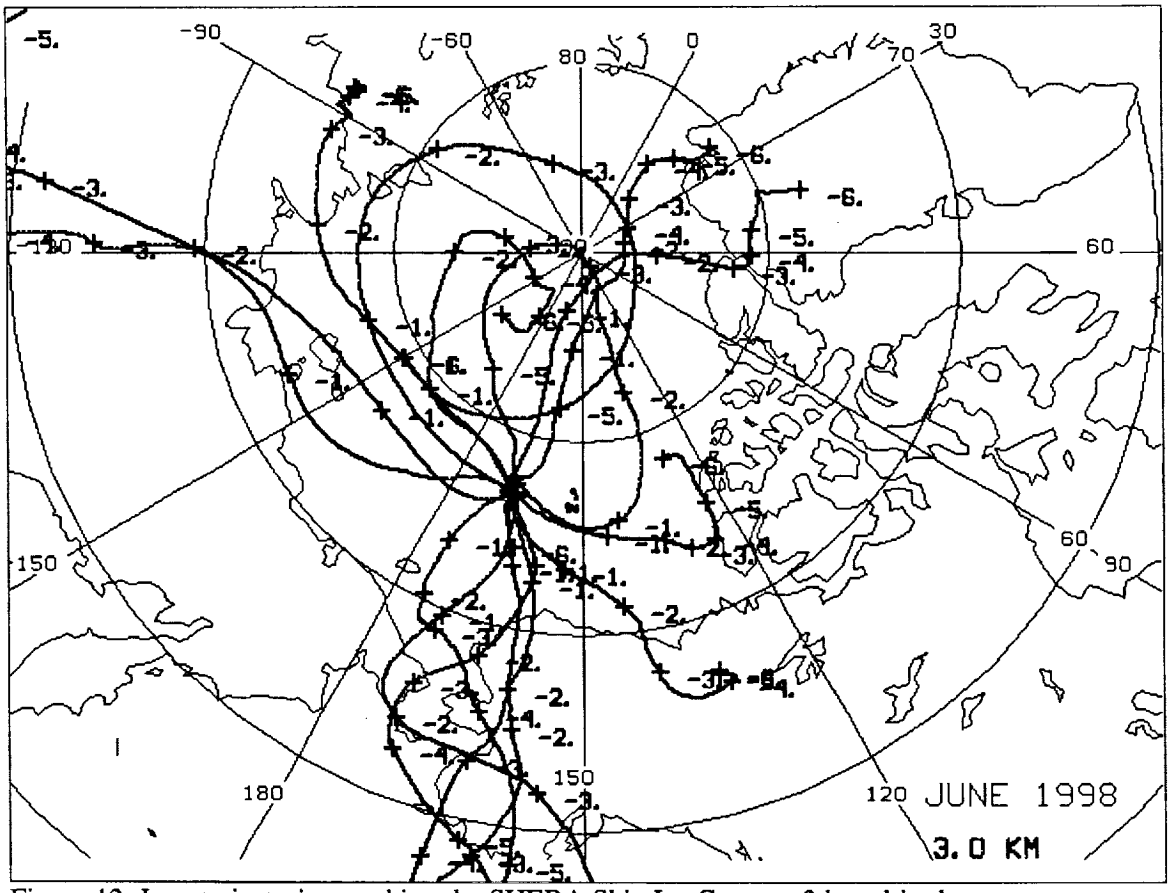

Figure 12: June trajectories reaching the SHEBA Ship Ice Camp at 3 km altitude.

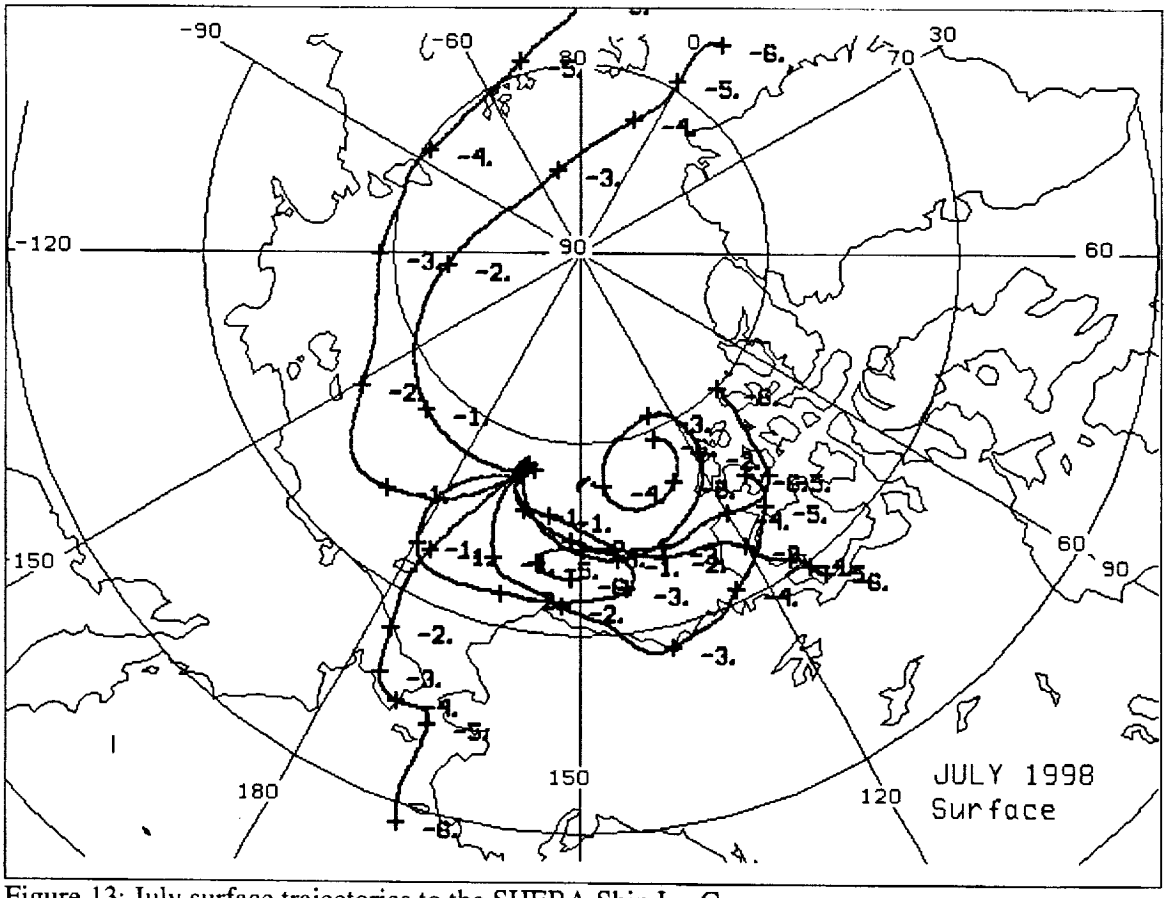

Figure 13: July surface trajectories to the SHEBA Ship Ice Camp.

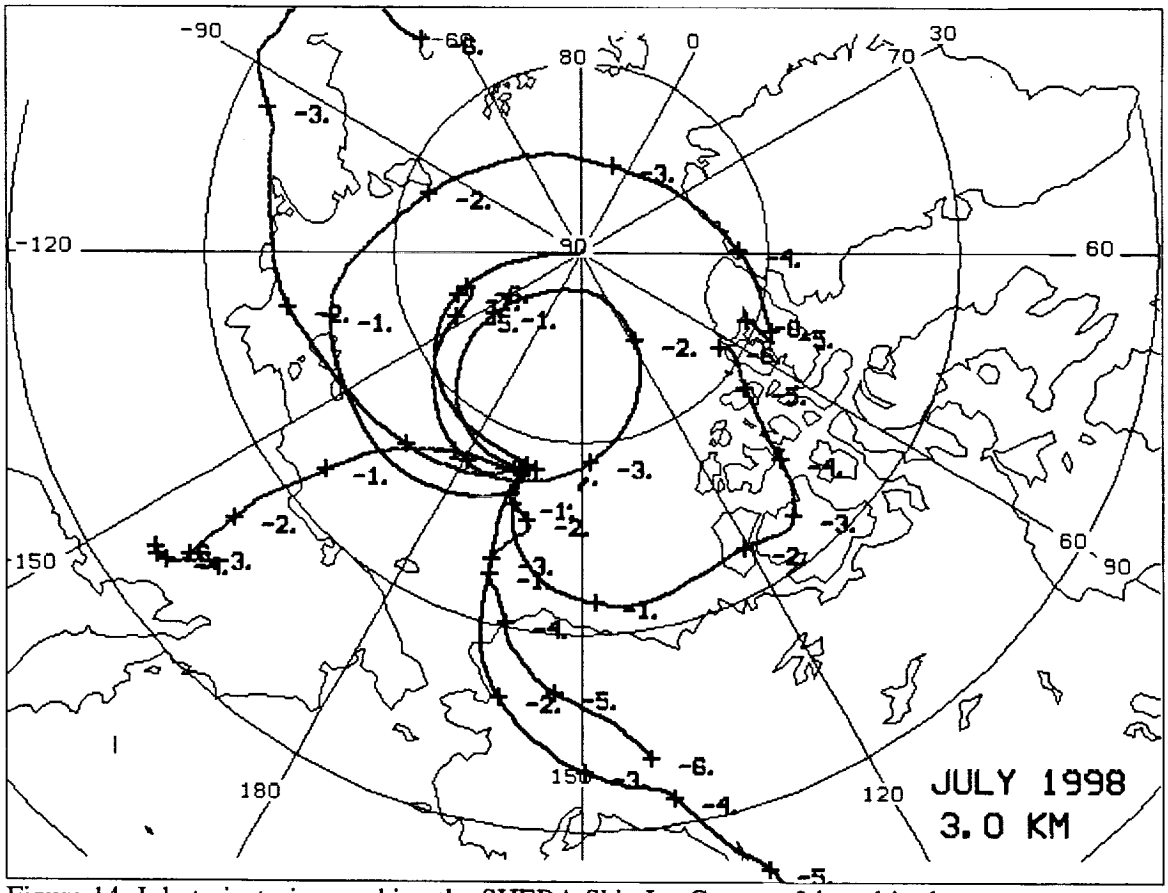

Figure 14: July trajectories reaching the SHEBA Ship Ice Camp at 3 km altitude.

Appendix B:

Effects of Long Range Transport and Clouds on Cloud Condensation Nuclei in the Springtime Arctic

Donald P. Wylie
Space Science and Engineering Center
University of Wisconsin-Madison
Madison, WI 53706

James G. Hudson
Desert Research Institute
Reno, NV
89512-1095

Submitted to the Journal of Geophysical Research
April 17, 2001

Abstract

Variations in cloud condensation nuclei (CCN) concentration vertical profiles during the FIRE/ACE flights over the Arctic Ocean were investigated using back trajectories and satellite photos. In contrast with CCN measurements over other oceans, concentrations over the Arctic generally increased with altitude. Although land masses did not seem to have as much of an immediate effect on concentrations over the Arctic as over other oceans, the small size of the Arctic Ocean may leave it open to greater overall continental/anthropogenic influences. Cloud scavenging seemed to be the most likely cause of decreased CCN concentrations. More efficient scavenging by liquid clouds, because of their higher concentrations and surface areas than cirrus clouds probably accounted for decreasing concentrations at lower altitudes.

1. Introduction

There has been increasing interest in cloud condensation nuclei (CCN) because higher concentrations from air pollution may be affecting global climate. Higher CCN concentrations can increase cloud albedo (Twomey, 1977; Kaufman et al., 1991; Wigley, 1991; Han et al. 1994) especially the globally significant widespread maritime stratus (Platnick and Twomey, 1994). The smaller cloud droplet sizes that follow from higher droplet concentrations can reduce coalescence precipitation (Albrecht 1989; Rosenfeld 2000; Hudson and Yum 2001; Yum and Hudson 2001a), which can result in greater cloud cover. Even apart from these indirect aerosol effects (Charlson et al., 1992) clouds remain the greatest uncertainty in models of global climate change (Arking 1991).

Since the Arctic Ocean seems to be especially sensitive to global change, the Surface Heat Budget in the Arctic (SHEBA) experiment (Perovich et al., 1999) was conducted in 1997-98. A central component of SHEBA was the maintenance of a research ship in the Arctic Ocean for more than a year. CCN concentrations were measured by aircraft flights over the SHEBA ship as part of the First International Satellite Cloud Climatology Project's Regional Experiment (FIRE) Arctic Cloud Experiment (FIRE/ACE, Curry, et al., 1999). This paper discusses the variations in CCN concentrations measured on the FIRE/ACE flights in May

1998. At low altitudes CCN concentrations (Yum and Hudson 2001b) were similar to those in apparently unpolluted air masses over other oceans (Hudson and Frisbie 1991; Hudson 1993; Hudson et al. 1998; Hudson and Xie 1999) (Fig. 1 and Table 1). At the very lowest levels where cloud scavenging seemed to be even more effective in the Arctic (Yum and Hudson 2001b) concentrations were lower than over other oceans. However, at higher altitudes concentrations over the Arctic Ocean were higher (Fig. 1 and Table 1) (Yum and Hudson 2001b; Ghan et al., 2001). The increase in concentrations with altitude over the Arctic (Table 1) is in sharp contrast with the relatively constant or decreasing concentrations with altitude over other apparently unpolluted oceans (Fig. 1). Table 1 excludes the immediate effects of direct scavenging in the lowest layers due to boundary layer clouds by excluding data at pressures above 900 hPa. The Arctic is the only project with a large negative slope (indicating increasing concentration with decreasing pressure) and it is the only project with a reasonably high correlation coefficient. Reasons for the variations in particle concentrations with altitude are sought from back trajectories of the air sampled during the flights and the clouds encountered during those trajectories.

2. Background

Hudson and Xie (1999) summarized CCN measurements over oceans from several experiments. They noted that CCN concentrations increased when the air came from continental sources within a few days of the measurements. Typical CCN concentrations were 100-300 cm^{-3} for oceanic air while continental air often raised CCN concentrations to ~1000 cm^{-3}. The largest changes were found in the northeastern Atlantic ocean where sources ranged from oceanic to the northwest to continental from Europe to the northeast (Hudson and Li 1995).

Typical concentrations of 200-300 cm^{-3} often decreased to less than 100 cm^{-3} in the boundary layer when clouds were present (Fig. 1). Twomey and Wojciechowski (1969), Hudson and Frisbie (1991), Hudson and Xie (1999), and Yum and Hudson (2001b) attribute the boundary layer decrease in CCN to cloud scavenging. This is mainly due to collision coalescence of larger cloud droplets. Whether these drops precipitate or evaporate they reduce CCN concentrations. Brownian diffusion of small interstitial particles is also especially efficient in clouds because of the large surface areas offered by the droplets (Hudson et al. 1998).

The Arctic Ocean is believed to be a region where aerosols and pollution are concentrated by advection from lower latitudes (Harris and Kahl, 1994; Rahn and Lowenthal, 1986; and Shaw, 1982). Air enters the arctic from lower latitudes in the circumpolar vortex where it sinks because of radiative cooling (Lorenz, 1967). Back trajectories of air usually lead to continental sources since the Arctic Ocean is one-sixth the size of the Atlantic and one-twelfth the size of the Pacific. Moreover, the Arctic is mostly surrounded by land, much of which has high human population densities. The Arctic also has a much lower tropopause, which leaves less room for dilution. Studies of chemical tracers by Jaffe et al. (1991) and Shaw (1982) have found anthropogenic sources of chemical pollutants from Europe to the Arctic.

The SHEBA ship was positioned in the western Arctic ocean at 76° north and 166° west during the May 1998 FIRE/ACE flights. The NCAR C-130 aircraft flew over the ship from Fairbanks AK (Curry et al., 1999). These flights collected condensation nuclei (CN; total particles) and CCN data between 30 m and 6.5 km using general flight patterns of a series of horizontal passes of ~40 km length over the SHEBA ship. Details of the CCN spectrometer are given by Hudson (1989) and of the Arctic CCN measurements by Yum and Hudson

(2001b). As in all previous presentations data obtained within clouds were excluded.

3. Characteristics of the vertical profiles

Average vertical profiles of CN and CCN at 3 different supersaturations (S) from FIRE/ACE are shown in Figure 2. As in Fig. 1 and in previous publications, the concentrations are normalized to standard pressure to discount the typical decrease in concentration with decreasing air density. The contrast between these average CCN profiles at S = 0.6% with those over other oceans is displayed in Fig. 1 and Table 1. With the exception of the boundary layer, where clouds often scavenged CCN to lower concentration levels, the Atlantic, Pacific, and Southern Ocean concentrations were quite constant with altitude or showed decreases with altitude. Arctic CCN concentrations, on the other hand, generally increased with altitude, with the largest concentrations observed at the highest levels that were measured, 450 hPa (6 km).

Vertical CCN profiles for each flight are then shown in Figure 3. In all flights the CCN concentrations were lowest in the boundary layer below 950 hPa (400 m) but especially when there were low stratus clouds of mostly liquid droplets (Yum and Hudson 2001b). There was considerable interflight variability in concentrations with the middle levels between 850 and 600 hPa (1.3-3.9 km) displaying the largest changes.

4. Reasons for CCN changes

To understand these variations in CCN concentrations, we examined back trajectories of air for 6 days prior to each measurement. These back trajectories were calculated on isentropic surfaces using the wind and temperature data from the National Oceanic and Atmospheric Administration's National Center for Environmental Prediction (NOAA/NCEP) global analysis. This analysis was produced twice per day. Back trajectories were calculated using one hour time increments and linear interpolation of the winds between the analyses times. These calculations are also summarized in Wylie (2001).

The **May 4** flight had the lowest CN and CCN concentrations averaged over all altitudes (Fig. 3a and Table 2). These lowest CCN concentrations of any of the flights were probably due to passage through convective clouds (Fig. 4) because a low pressure system was approaching the ship from the northwest. This system eventually merged with a second low that traveled north into the Beaufort Sea east of the ship. Thus air sampled on the May 4 flight had traveled in a large cyclonic gyre that approached the ship from the west. The air at higher levels traced back around the cyclonic gyre to near the pole (3 and 6 km trajectories Fig. 4). Clouds can be seen on satellite images west of the ship for three days and the trajectories indicated that the air had passed through them. The radar on the SHEBA ship reported cellular clouds reaching up to 5.5 km (480 hPa) on May 4. The relative humidity profiles from ship-launched rawinsondes also indicated possible clouds up to the tropopause at 360 hPa (7.3 km). Satellite infrared images found thin cirrus clouds up to 8.5 km (300 hPa). The reason for the low CCN concentrations is thus probably cloud scavenging. Only the highest flight legs at 560-540 hPa (4.3-4.6 km) recorded CCN >300 cm^{-3}. This air probably experienced less liquid cloud. Liquid clouds are probably more efficient scavengers of CCN because the higher concentrations cause more nucleation of CCN. Moreover the greater surface area of the droplets compared to larger ice crystals in cirrus clouds are a result of more Brownian scavenging of interstitial particles (particles that are CN but not CCN).

The **May 7** flight reported higher CCN concentrations than the previous flight at nearly all altitudes. The only exceptions

being very close to the surface and at 860 and 710 hPa where there were some narrow concentration peaks on May 4. Above 700 hPa (2.8 km) there was a steady increase from 230 to 500 cm^{-3} at 450 hPa (5.9 km) and then to 600 cm^{-3} at 410 hPa (6.5 km). This air came from different places (Fig 5) than the previous flight. The lower level air, surface to 1 km, came from the Chukchi sea to the south. Low level winds were light. The upper levels, 3 and 6 km trajectories show air coming from the southwest – Siberia. Clouds were mostly absent along the back air trajectories except for the boundary layer arctic stratus clouds. The arctic stratus clouds appeared to be diffuse and within 1 km of the surface. Patterns in the ice could easily be seen through them on satellite images. The exact height of these clouds could not be determined from satellite data because of the low level temperature inversion. The absence of clouds above 1 km along the air trajectories implies that cloud scavenging didn't affect the CCN concentrations except for the lowest 0.1 km in the arctic stratus clouds. This is why those concentrations were generally lower than flight 1 (May 4).

The **May 11** flight found even higher CCN concentrations that approached 400 cm^{-3} above 810 hPa (1.6 km). The layer from 810 to 590 hPa (1.6-4.0 km) had distinctly more CCN than the previous flights. There were distinctly higher concentrations of the low S CCN. Since these are the most water soluble (generally larger) particles this might indicate a lack of cloud encounters. Above 590 hPa (4 km) CCN concentrations were much more variable, ranging from 140 to 500 cm^{-3}, the latter was similar to the previous flight. The low concentrations associated with boundary layer clouds seemed to extend to higher altitudes than the previous two flights especially compared to the flight of May 7. The low level air, surface to 1.0 km, had a cyclonicly curved trajectory from the east into the Beaufort Sea (Fig 6). Satellite images show clouds in the Beaufort and Chukchi Seas between 747 and 613 hPa (2.3-3.8 km) for four days. Snow was reported at the ship for 24 hours before the flight. The low CCN concentrations from the surface to 900 hPa (0.8 km) were probably caused by immediate cloud scavenging.

A low pressure system was moving into the Beaufort Sea from Alaska on a track east of the SHEBA ship. Three days before the flight a large high pressure system dominated most of the Beaufort Sea east of the ship.

The mid-troposphere trajectories between 826 and 600 hPa (1.5-3.9 km) came from the west. Winds were light so the air only traveled 550 km in four days (Fig. 6). Cloud cover appeared on the satellite images for four days before this flight west of the SHEBA ship with tops ranging from 613 to 532 hPa (3.8-4.8 km). Lower CCN concentrations would have been expected because of scavenging within the clouds. However, the trajectory calculations also show that the air descended as much as 250 hPa (2.9 km) in its eastward path to the ship. The trajectory with the largest descent was at 750 hPa (2.3 km) altitude, which came from 500 hPa (5.2 km) at a horizontal distance of 600 km west of the ship. This is a large descent because air from the south typically descended only 62 hPa (0.7 km) in a 6 day track to the SHEBA ship. The large descent of the mid-level air on May 11 is incompatible with sustaining clouds. Cloud scavenging probably did not occur since any cloud probably evaporated at this level. Since CCN concentrations typically increased with altitude in all profiles, the air sampled between 826 and 600 hPa (1.5-3.9 km) probably brought high CCN concentrations down from higher altitudes of (i.e., 500 hPa) to the west.

Above 600 hPa (3.9 km) air seemed to have come from the south, the Bering Straight where numerous high clouds were evident on the satellite images. The presence of these clouds is probably the reason for highly variable CCN concentrations. Where low concentrations were found, the CCN were probably scavenged by cloud formation. Since this cloud field contained many breaks and elongated features, the

flight legs measuring higher CCN concentrations were probably in air that had missed most of the clouds.

The **May 15** flight found a somewhat similar CCN vertical profile to the May 11 flight. At the lowest flight level, 0.15 km, the CCN concentrations were the lowest up to that date in FIRE/ACE--50 cm^{-3} (only flight 8 on May 27 had lower concentrations). The low level trajectories from the surface to 860 hPa (1.3 km) came from the east, the Beaufort Sea and the Canadian Archipelago (Fig. 7). Dense low clouds were seen in satellite images of this area with tops up to 650 hPa (3.3 km). The clouds were organized into elongated fields with large clear areas in between. The SHEBA ship radar reported clouds up to 800 hPa (1.8 km) during the flight. Scavenging of CCN by clouds probably accounted for the low concentrations near the surface.

Trajectories above 840 hPa (1.5 km) came from Alaska to the southeast. Cloud cover was minimal in the Beaufort Sea with some small elongated cloud fields with tops of 655 hPa (3.3 km). The peak concentration at 800 hPa is associated with a second inversion that was found at about 830 hPa; layers above temperature inversions are usually cloud free and this means a lack of scavenging. Minimal concentrations between 660 and 560 hPa are probably a result of cloud scavenging because a sounding just before the flight showed a moist layer between 650 and 580 hPa. Faint cloud can also be seen on satellite images, which definitely show cloud upstream. Above this level there were higher concentrations, especially of CN (more than 900 cm^{-3}) and low S CCN. Higher altitude trajectories, 450 hPa (6.0 km) trace back to the northwest, initially, and then curved to the south, the Bering Straight. This route appeared to be mostly cloud free on satellite images.

The **May 18** flight found the same very low CCN concentrations of 50 cm^{-3} and CN concentrations of 70 cm^{-3} in the lowest flight legs. However, there was a very sharp vertical gradient to 200 cm^{-3} at 960 hPa (0.2 km). Above 960 hPa, concentrations showed a vertical pattern that was similar to the previous flights but the concentration extremes were not as great; i.e., the flatter 300 cm^{-3} peak at approximately 810 hPa and the flatter 170 cm^{-3} minimum at 660 hPa contrasts with the narrow maximum and minimum of 100 cm^{-3} at these same altitudes for the previous flight. Above 550 hPa concentrations were lower than the previous flight.

Air trajectories came from a variety of directions (Fig. 8) for May 18. Low level air came from the east, the Beaufort Sea. These trajectories also curved north into the Arctic Ocean through patches of low clouds. Satellite images show these cloud tops to be 680 hPa (3.1 km) in the northern Beaufort Sea. Low clouds were also present over the ship during the flight. The 700 hPa (3 km) trajectory curves to the west where similar low clouds appeared on the satellite image with similar heights to those of the northern Beaufort Sea.

The 600 hPa (4.1 km) trajectory traces directly south to the Bering Straight. Higher altitude trajectories also start tracing south but then curve to the northwest. The 600 hPa (4.1 km) trajectory deviates from the other altitudes by not curving back to the north. The CCN concentration at 560 hPa (4.1 km) rose to 400 cm^{-3}, which is slightly higher than that above and below this level. The reason for this narrow peak is probably the different source of the air at 600 hPa. Numerous high clouds are seen on the satellite images south of the SHEBA ship with heights of 490 hPa (5.6 km). Scavenging of CCN was possible for the 600 hPa trajectory, however, these are cirrus clouds, which do not scavenge CCN as well as liquid phase clouds.

On **May 20** the CCN concentrations in the lowest flight legs were much higher--200 cm^{-3} --because of the absence of low clouds (Yum and Hudson 2001b). Above the boundary layer there was a gradual irregular increase up to 500 hPa (5.6 km) where concentrations were 500 cm^{-3}, with the exception of a narrow peak of 1300 cm^{-3}. The trajectories at all levels were spirals near the ship in the Chukchi and Beaufort

Seas (Fig. 9). Satellite images indicate some low level cloud cover that reached 618 hPa (3.9 km) in a few areas. The ship radar indicated only a few low level clouds with clearing 20 hours before the flight. Scavenging of CCN by clouds appears to be minimal at all levels.

On **May 24** the vertical CCN pattern was similar to the previous flight. At the lowest levels the concentrations were even higher than the previous flight, as these were the only flights without low level clouds. Above the boundary layer and below 700 hPa, concentrations were slightly lower and much less variable with altitude. Above 700 hPa there was a much sharper and more regular increase with altitude to 600 cm^{-3} at 490 hPa. Above that level concentrations were variable. The air trajectories show local spirals near the ship at all levels (Fig. 10). This area also was nearly cloud free for 2.5 days. Light cirrus clouds were identified on satellite images northwest of the ship from 7-10.1 km. The ship radar reported broken clouds from 6-8 km on May 21 and 22. Lower cloud layers were not seen by the ship's radar for 2.5 days before the flight. However, the satellite images show cirrus clouds from 6.5-10.1 km north and northeast of the ship, which the air trajectories passed through 1 day prior to the flight.

On **May 27** the return of low level clouds drastically reduced the lowest level CCN concentrations from the previous flight to only 20-50 cm^{-3}. Between 920 and 700 hPa concentrations were higher and more irregular with altitude than the previous two flights. In fact this flight showed the most variability in concentrations especially between adjacent altitudes. After a dip to 200 cm^{-3} at 630 hPa, similar to flight 4, there was a sharp gradient to 500 cm^{-3} at 590 hPa. Above that altitude concentrations were irregularly high where they were more similar to flight 6 and lower than flight 7. Trajectories show all air at all levels coming from the south through dense cloud cover (Fig. 11). The ship radar reported clouds from the surface to 9.5 km before the flight. The satellite images show a variety of heights up to 10.3 km. These clouds also appear to be convective on the satellite images so scavenging of CCN is most likely responsible for the lower CCN concentrations.

The CCN concentrations on May 27 between 600 and 500 hPa (4.1-5.5 km) were slightly higher than other flights where high cloud cover was definitely found along the air trajectory path to the ship, such as May 4 and 15. May 27 found CCN concentrations of 300-710 cm^{-3} while the other two flights found only 150-380 cm^{-3} in this layer.

Table 2 summarizes the vertically averaged CCN concentrations at 1% and 0.1% supersaturation between 900 hPa (0.85 km) and 500 hPa. The CCN at 0.1% supersaturation are larger and/or more hygroscopic particles compared to the 1% particles.. Hudson et al. (1998) found that the larger CCN appeared to be more affected by cloud scavenging than the smaller particles as they are more likely to be within cloud droplets and within larger cloud droplets (Twohy and Hudson, 1995), which are more likely to coalesce. On the other hand there is the competing effect that coalescence can increase lower S CCN concentrations by putting nuclei together from the coalescing droplets (Hudson and Frisbie 1991).

Table 2 seems to suggest an increase in total (1% S) CCN concentrations throughout the month. But the decrease in the concentrations of the 0.1% CCN through the month is more apparent. Linear regressions of concentration with date show much higher correlations for the decrease of the 0.1% nuclei. If only the flights with clouds (especially low clouds) are considered (excluding flights 6 and 7 on 20 and 24 May) then there is no time trend for 1% concentrations. There is, however, a correlation coefficient of 0.80 for the linear regression decrease of the 0.1% S CCN at a rate of 3.5 particles per day. Even with only these 6 data points this linear regression has a 97% significance level. This then denotes an increase in the concentrations of small CCN (the difference in the 1% and 0.1% S concentrations). The decrease in the concentration of the most active CCN

throughout the month of May may be associated with the increase in cloudiness especially low cloudiness that is a more common feature over the Arctic Ocean in summer. Moreover, there is certainly an increase in temperature, which would make for more liquid phase clouds, which more efficiently scavenge CCN.

5. Summary and conclusions

5a. The arctic stratus clouds in the boundary layer appear to have lowered the CCN. The vertical profiles of CCN from FIRE/ACE show distinctly lower values in the boundary layer than other oceanic data reported by Hudson and Xie (1999). This is surprising since the arctic stratus clouds are diffuse, have low optical depths, and light precipitation.

5b. Lower CCN concentrations were commonly found in air that had passed through all forms of clouds except cirrus.

5c. Cirrus clouds seem to have a variable affect on CCN. Large variances in CCN concentrations were found when Ci were up stream in the air back trajectories.

5d. Cloud scavenging decreased the CN and CCN concentrations at all supersaturations.

5e. The large increases in CCN in air coming directly from continents seen in the Atlantic and Pacific oceans by Hudson and Xie (1999) and Hudson and Yum (2001) were not found in the Arctic ocean. The highest CCN concentrations were measured in air that resided in the Arctic ocean for at least 6 days without recent encounters with clouds.

5f. The vertical profiles of CCN in the Arctic ocean were different from other oceanic data. The highest concentrations were found at the highest flight levels measured, 450 hPa (6.5 km) on each flight. This is at or near the tropopause. Other CCN measurements in the north Atlantic and Pacific oceans found maximum CCN values in the lower troposphere just above boundary layer clouds. The low altitude maxima in other oceans probably results from CCN entering the atmosphere from the surface and then mixing vertically. Scavenging by boundary layer clouds often removes many of the lowest level CCN leaving a maximum in CCN just above the boundary layer clouds over the other oceans (e.g., Hudson and Frisbie 1991). The different CCN vertical profile in the Arctic ocean probably results from CCN traveling longer distances than the 6 day back trajectories used here indicated. The accuracy of the available wind data limited back trajectories to 6 days. CCN are probably advected into the Arctic ocean at many levels and reside there until removed by cloud scavenging. Lower tropospheric clouds are very common in the Arctic (Wylie, 2001) especially during the summer season and they probably remove many of the CCN in the lower troposphere. Upper tropospheric clouds are usually broken and thin cirrus. Since they remove fewer CCN than the lower cloud forms this leaves a vertical profile with low CCN in the boundary layer and adjacent layers that are also affected, and maximum concentration near the tropopause. The close proximity to strong continental/anthropogenic sources, the small size of the Arctic basin, and the shallow troposphere probably allow relatively greater inputs of particles over the Arctic Ocean than over other oceans. The lower percentage of liquid phase clouds especially at higher altitudes and the more limited vertical mixing probably allow the higher CCN concentrations at higher altitudes.

6. Acknowledgements

This work was supported by grant NAG-1-2196 from the National Aeronautics and Space Administration.

7. References

Albrecht, B. A., Aerosols, cloud microphysics, and fractional cloudiness, *Science, 245,* 1227-1230, 1989.

Arking, A., The radiative effects of clouds and their impact on climate, *Bull. Amer. Meteorol. Soc., 72,* 795-813, 1991.

Charlson, R. J., S. E. Schwartz, J. M. Hales, R. D. Cess, J. A. Coakley Jr., J. E. Hansen, and D. J. Hofmann, Climate forcing by anthropogenic aerosols, *Science, 255,* 423-430, 1992.

Curry, J. A., and 26 Coauthors, FIRE arctic cloud experiment, *Bull. Amer. Meteor. Soc., 81,* 5-28, 1999.

Ghan, S.J., R.C. Easter, J. Hudson, and F.-M. Breon, Evaluation of aerosol indirect radiative forcing in MIRAGE, *J. Geophys. Res., 106,* 5317-5334, 2001.

Han, Q., Rossow, W.B., and A.A. Lacis, Near-global survey of effective droplet radii in liquid water clouds using ISCCP data. *J. Climate* **7**, 465-497, 1994.

Harris, J. M., and J. D. W. Kahl, Analysis of 10-day isentropic flow patterns for Barrow, Alaska: 1985-1992., *J. Geophy. Res., 99,* 25,845-25,855, 1994.

Hudson, J. G., An instantaneous CCN spectrometer, *J. Atmos. Oceanic Tech., 6,* 1055-1065, 1989.

Hudson, J.G., and P.R. Frisbie, Cloud condensation nuclei near marine stratus, *J. Geophys. Res., 96,* 20,795-20,808, 1991.

Hudson, J. G., Cloud condensation nuclei, *J. Appl. Meteorol., 32,* 596-607, 1993.

Hudson, J.G., and H. Li, Microphysical contrasts in Atlantic stratus, *J. Atmos. Sci.*, 52, 3031-3040, 1995.

Hudson, J. G., Y. Xie, and S. S. Yum, Vertical distributions of cloud condensation nuclei spectra over the summertime Southern Ocean, *J. Geophys. Res., 103,* 16,609-16,624, 1998.

Hudson, J. G., and Y. Xie, Vertical distributions of cloud condensation nuclei spectra over the summertime northeast Pacific and Atlantic Oceans, *J. Geophys. Res., 104,* 30,129-30,229, 1999.

Hudson, J.G., and S.S. Yum, Maritime/continental drizzle contrasts in small cumuli, *J. Atmos. Sci.*, **58,** 915-926, 2001.

Jaffe, D. A., R. E. Honrath, J. A. Herring, S. M. Li, and J. D. Hahl, Measurements of nitrogen oxides at Barrow, Alaska during spring: Evidence for regional and northern hemispheric sources of pollution, *J. Geophys. Res., 96,* 7,395-7,405, 1991.

Kaufman, Y. J., R. S. Fraser, and R. L. Mahoney, Fossil fuel and biomass burning effect of climate heating or cooling, *J. Clim., 4,* 578-588, 1991.

Lorenz, E. N., The nature and theory of the general circulation of the atmosphere, *World Meteor. Organization, WMO No. 218.TP.115,* 161 pp., 1967.

Perovich, D. K., and Coauthors, Year on ice gives climate insights, *EOS, Trans. Amer. Geophys. Union, 80,* 481, 1999.

Platnick, S., and S. Twomey, Determining the susceptibility of cloud albedo to changes in droplet concentration with the advanced very high resolution radiometer, *J. Appl. Meteorol., 33,* 334-347,1994.

Rahn, K. A., and D. H. Lowenthal, Who's polluting the Arctic? Why is it so important to know? An American perspective. *In Arctic air pollution, ed. B. Stonehouse, Cambridge Univ. Press,* 85-96, 1986.

Rosenfeld, D., Suppression of rain and snow by urban and industrial air pollution, *Science, 287,* 1793-1796, 2000.

Shaw, G. E., 1982: Evidence for a Central Eurasian source area of Arctic Haze in Alaska., *Nature, 299,* 815-818, 1982.

Twohy, C. H., and J.G. Hudson, Cloud condensation nuclei spectra within maritime cumulus cloud droplets, *J. Appl. Meteorol., 34,* 815-833, 1995.

Twomey, S., and T. A. Wojciechowski, Observations of the geographical variations of cloud nuclei, *J. Atmos. Sci., 26,* 684-688, 1969.

Twomey, S., The influence of pollution on the shortwave albedo of clouds, *J. Atmos. Sci., 34,* 1149-1162, 1977.

Wigley, T. M. L., Could reducing fossil-fuel emissions cause global warming?, *Nature, 349,* 503-506, 1991.

Wylie, D. P., Arctic weather during the FIRE/ACE flights in 1998, *J. Geophys. Res.*, in press, 2001.

Yum, S.S., and J.G. Hudson, Maritime/continental microphysical contrasts in stratus, *Tellus,* in review, 2001a.

Yum, S. S., and J. G. Hudson, Vertical distributions of cloud condensation nuclei spectra over the springtime Arctic Ocean, *J. Geophys. Res.*, in press 2001b.

Tables

Table 1. Linear regressions of CCN concentration cm^{-3} at 0.6% S corrected to standard pressure versus pressure altitude in hPa for averages of the five projects over the four oceans shown in Figure 1. Only data between 500 and 900 hPa are used for these regressions. Columns 2 and 3 show the intercept of these regressions at 500 and 900 hPa. The latter is just above the boundary layer. Negative slopes mean increasing concentrations with decreasing pressure (increasing concentration with altitude). Row 1 is from Yum and Hudson (2001b), rows 2, 3, and 4 are from Hudson and Xie (1999), and row 5 is from Hudson and Yum (2001). For the last two rows only data in the maritime portions of these projects is used.

Project	Concentration (cm^{-3}) @ 500 hPa	Concentration (cm^{-3}) @ 900 hPa	Slope	Correlation coefficient
Arctic	321	173	-0.37	-0.77
Southern	198	162	-0.09	-0.54
Pacific	161	133	-0.07	-0.30
E. Atlantic	118	270	+0.38	+0.73
W. Atlantic	294	322	+0.07	+0.51

Table 2: CCN concentrations averaged between 900 hPa (0.85 km) and 500 hPa (5.6 km) for 0.1% and 1.0% supersaturations.

Flight Date	CCN concentration 0.1% S	1.0% S	Comments
May 4	119	203	All air from gyre in arctic, but passed through clouds
May 7	163	234	Air above B.L. had no clouds. 6 km air from Siberia
May 11	110	278	Air from Bering Straight except for middle levels, which had strong descent
May 15	97	211	Air passed through clouds from east and south
May 18	68	212	Surface to 4 km air came through clouds in Arctic, 6 km air did not encounter cloud.
May 20	86	297	All air from local gyres in arctic. No clouds encountered.
May 24	121	308	Similar to 20 May. No clouds encountered.
May 27	58	236	All air from the south with numerous convective clouds

List of figures

Figure 1: Average cloud condensation nuclei (CCN) concentrations (0.6% supersaturation) from five different experiments.

Figure 2: Average CCN concentrations measured at three levels of supersaturation along with Condensation Nuclei concentrations in the FIRE/ACE flights.

Figure 3: Vertical profiles of CCN concentrations (1% supersaturation) measured during each FIRE/ACE flight. The large dots are the average for a flight level while the error bars show the variance.

Figure 4: Back trajectories to the SHEBA ship for the air sampled on the May 4, 1998 flight. The bold numbers are the number of days prior to reaching the ship. The satellite image is from three days prior to the May 4 flight.

Figure 5: Back trajectories for the air sampled on the May 7, 1998 flight. The satellite image is from 18 hours prior to the flight.

Figure 6: Back trajectories for the air sampled on the May 11, 1998 flight. The satellite image is from 2 days prior to the flight.

Figure 7: Back trajectories for air sampled during the May 15, 1998 flight. The satellite image is from 4 days prior to the flight.

Figure 8: Back trajectories for air sampled on the May 18, 1998 flight. The satellite image is from 2 days prior to the flight.

Figure 9: Back trajectories for air sampled on the May 20, 1998 flight. The satellite image is from 1 day prior to the flight.

Figure 10: Back trajectories for air sampled on the May 24, 1998 flight. The satellite image is from 2 days prior to the flight.

Figure 11: Back trajectories for air sampled on the May 27, 1998 flight. The satellite image is from 1 day prior to the flight.

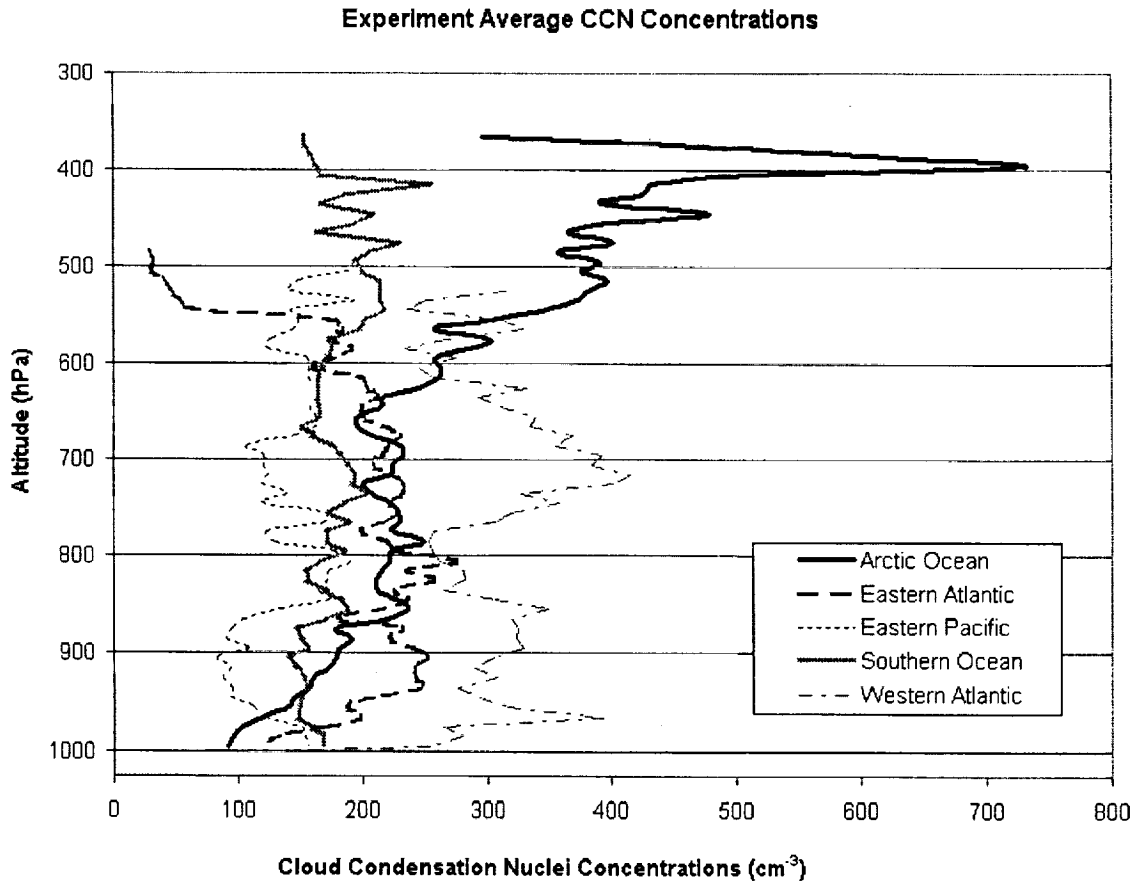

Figure 1: Average cloud condensation nuclei (CCN) concentrations (0.6% supersaturation) from five different experiments.

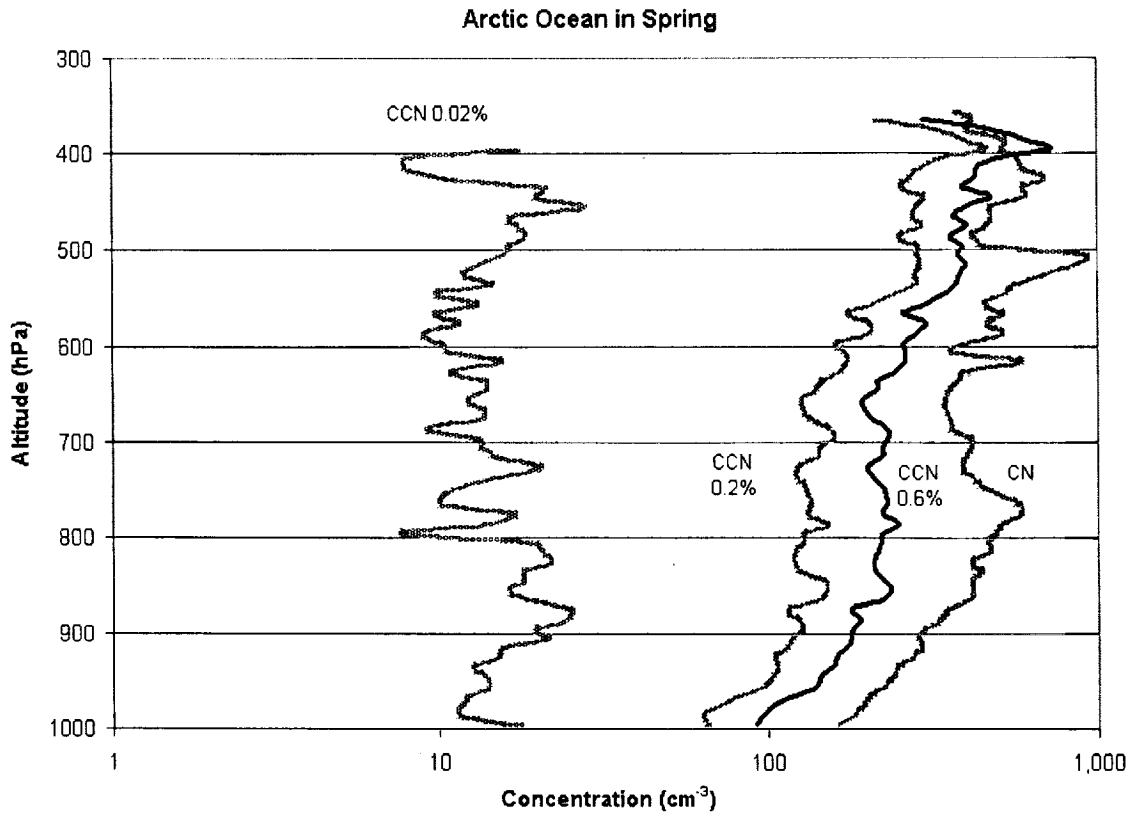

Figure 2: Average CCN concentrations measured at three levels of supersaturation along with Condensation Nuclei concentrations in the FIRE/ACE flights.

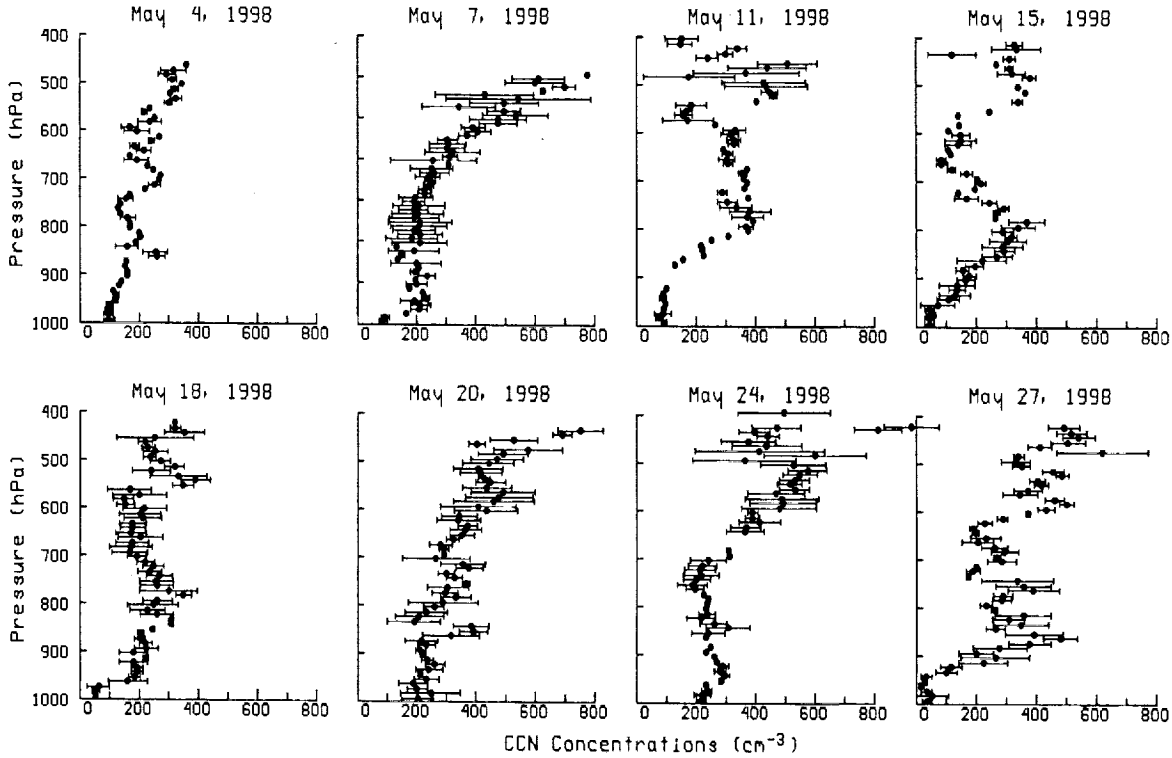

Figure 3: Vertical profiles of CCN concentrations (1% supersaturation) measured during each FIRE/ACE flight. The large dots are the average for a flight level while the error bars show the variance.

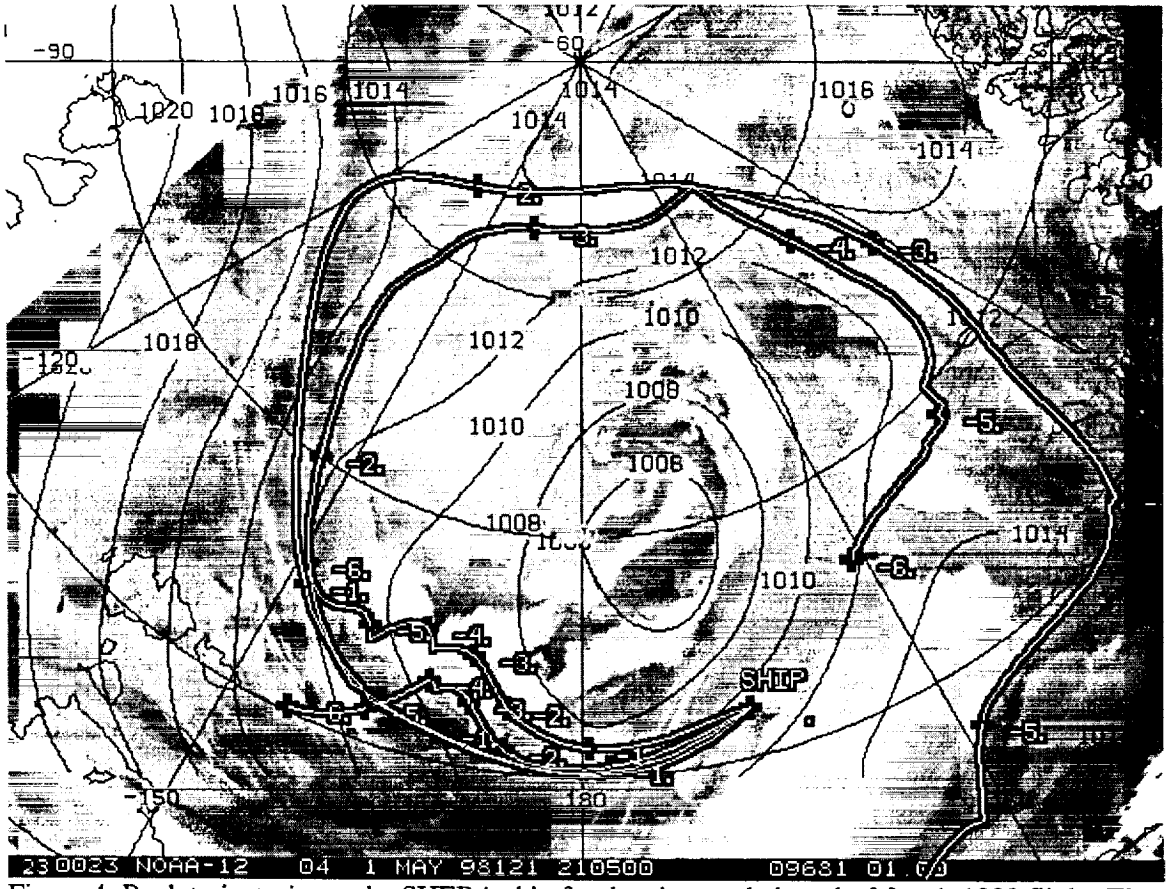

Figure 4: Back trajectories to the SHEBA ship for the air sampled on the May 4, 1998 flight. The bold numbers are the number of days prior to reaching the ship. The satellite image is from three days prior to the May 4 flight.

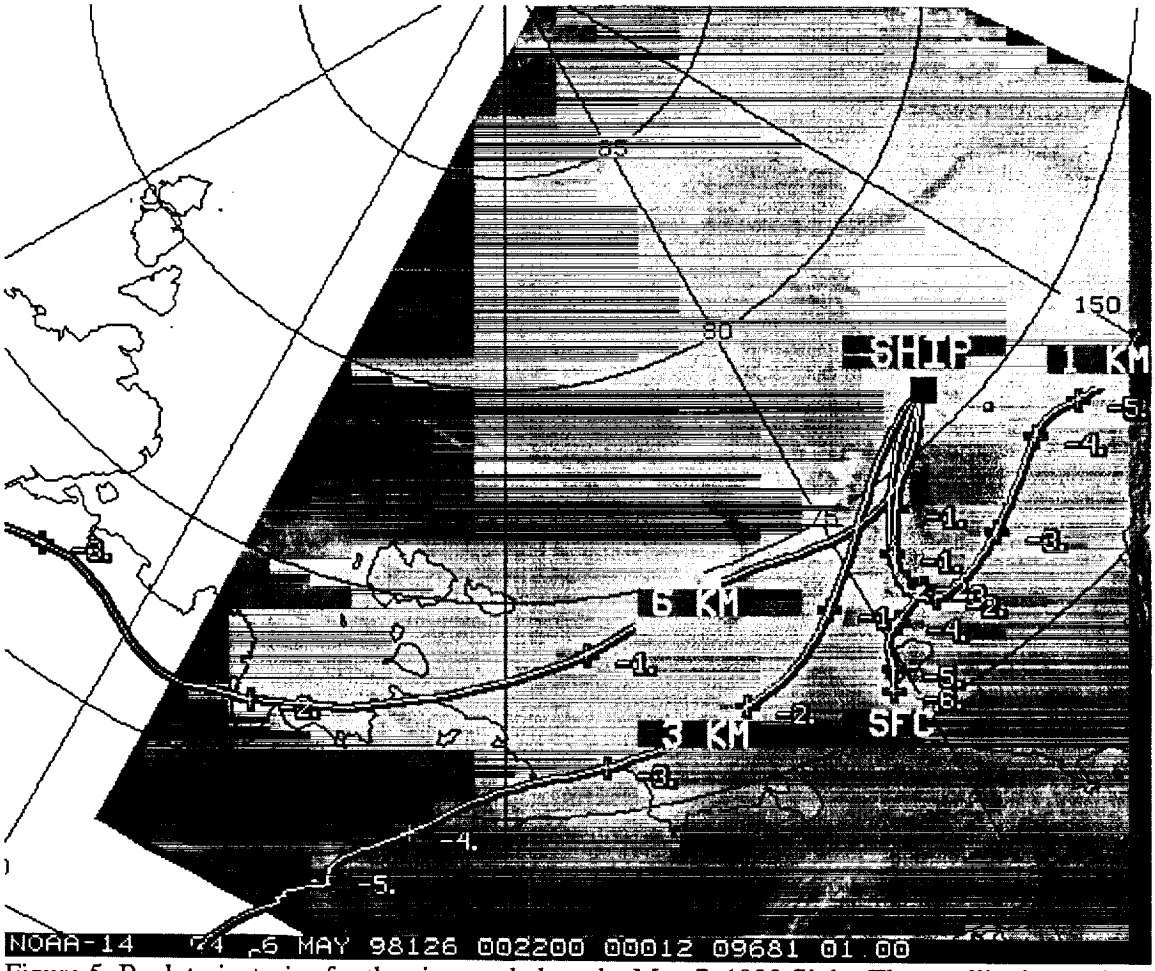

Figure 5: Back trajectories for the air sampled on the May 7, 1998 flight. The satellite image is from 18 hours prior to the flight.

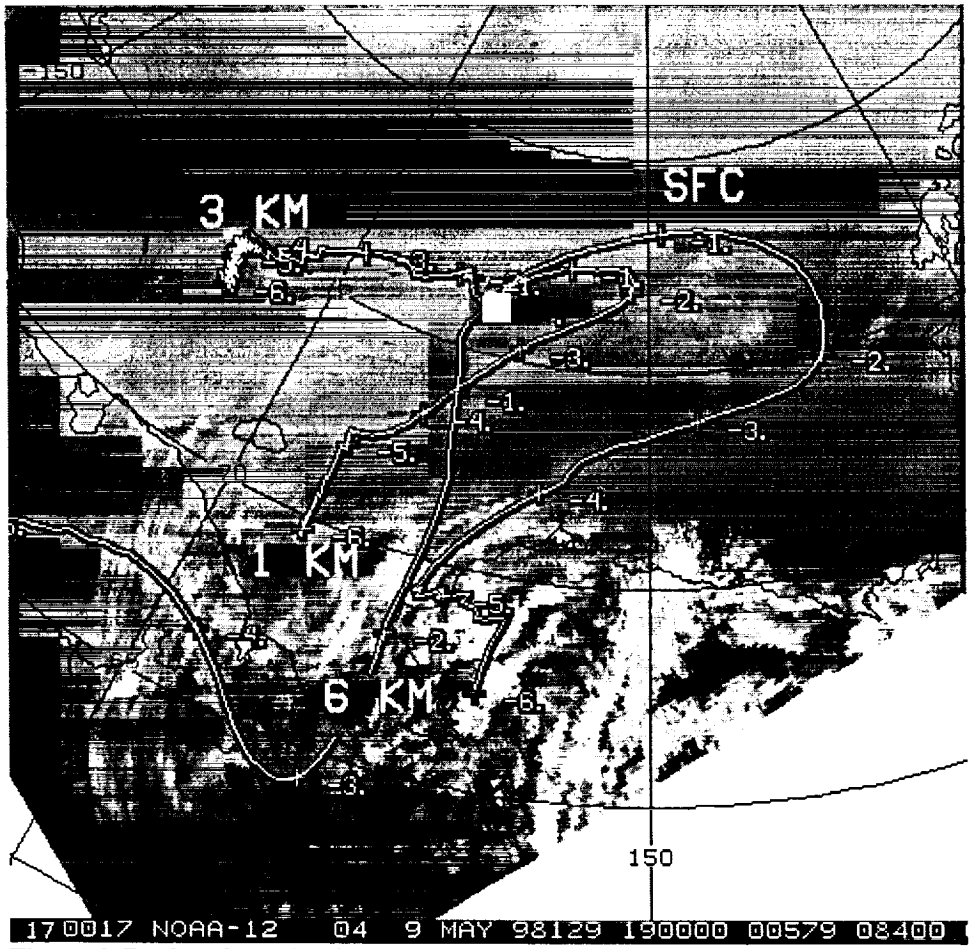

Figure 6: Back trajectories for the air sampled on the May 11, 1998 flight. The satellite image is from 2 days prior to the flight.

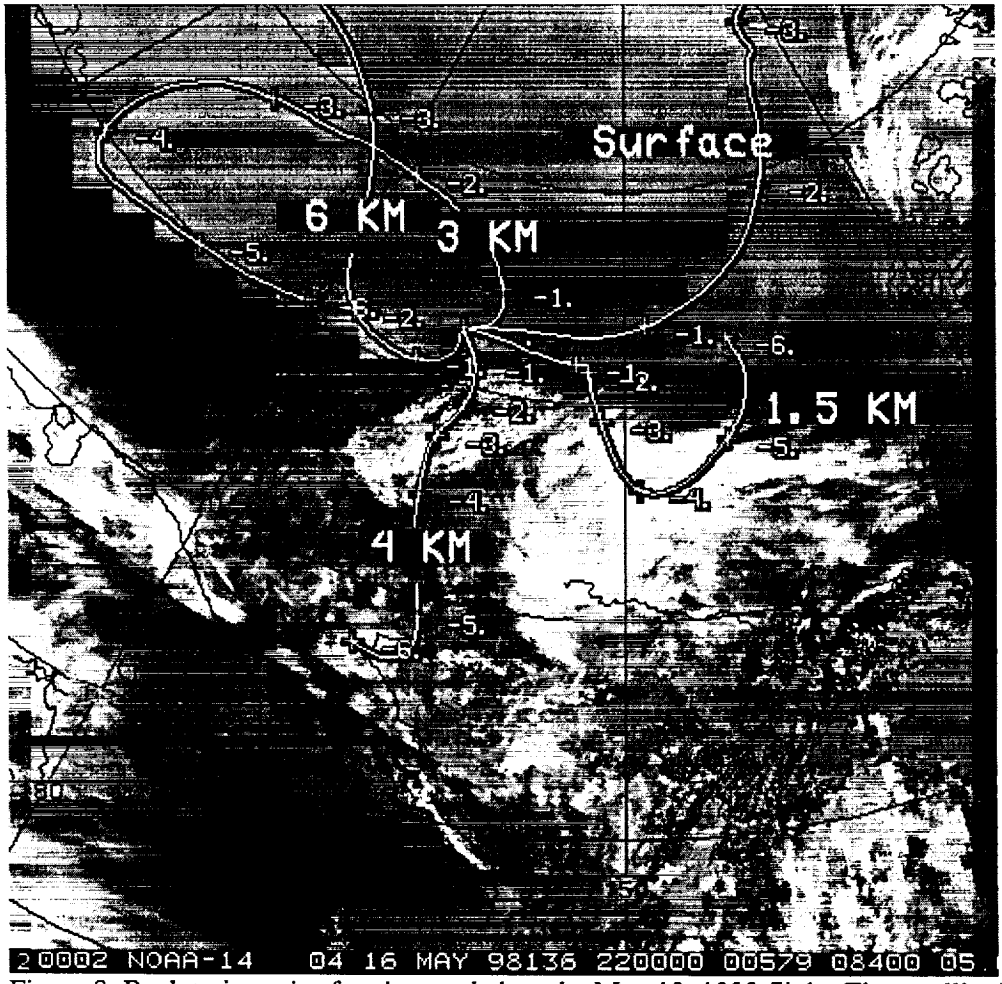

Figure 8: Back trajectories for air sampled on the May 18, 1998 flight. The satellite image is from 2 days prior to the flight.

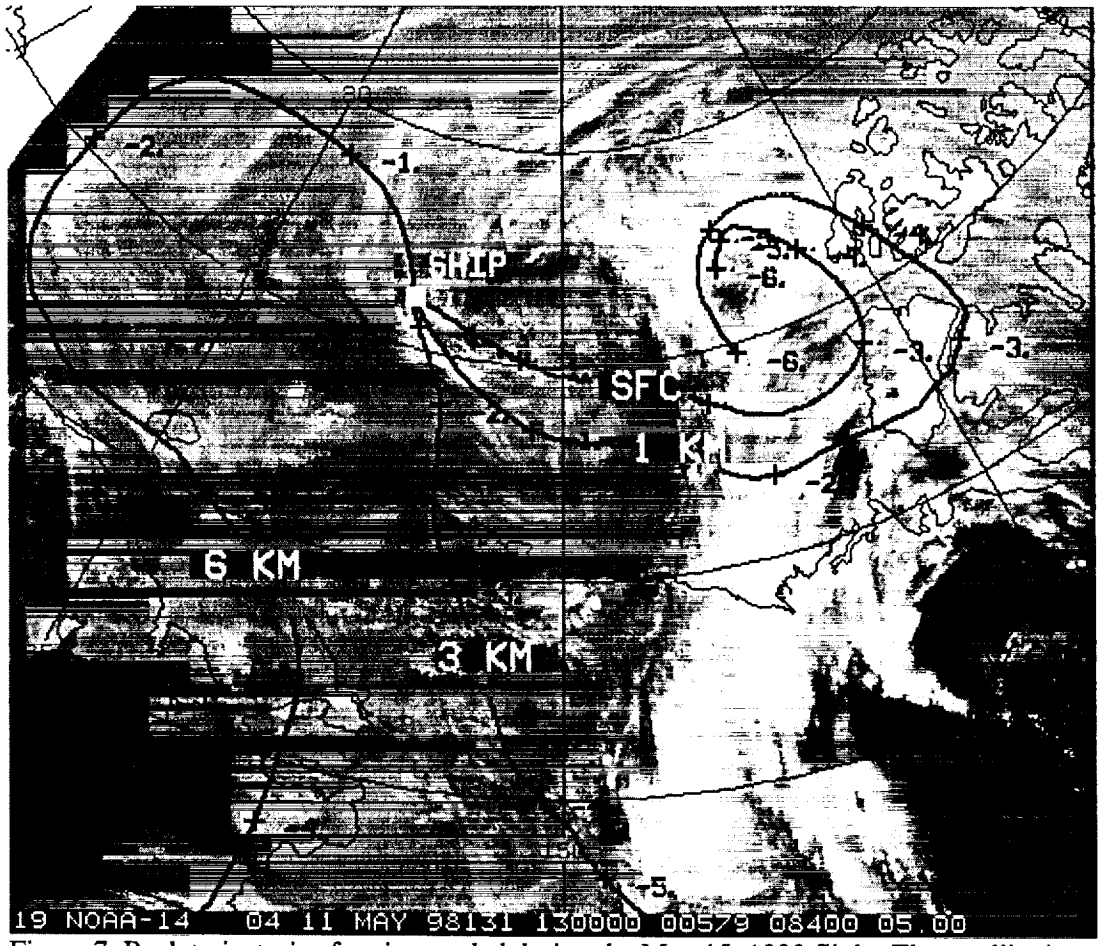

Figure 7: Back trajectories for air sampled during the May 15, 1998 flight. The satellite image is from 4 days prior to the flight.

Figure 9: Back trajectories for air sampled on the May 20, 1998 flight. The satellite image is from 1 day prior to the flight.

Figure 10: Back trajectories for air sampled on the May 24, 1998 flight. The satellite image is from 2 days prior to the flight.

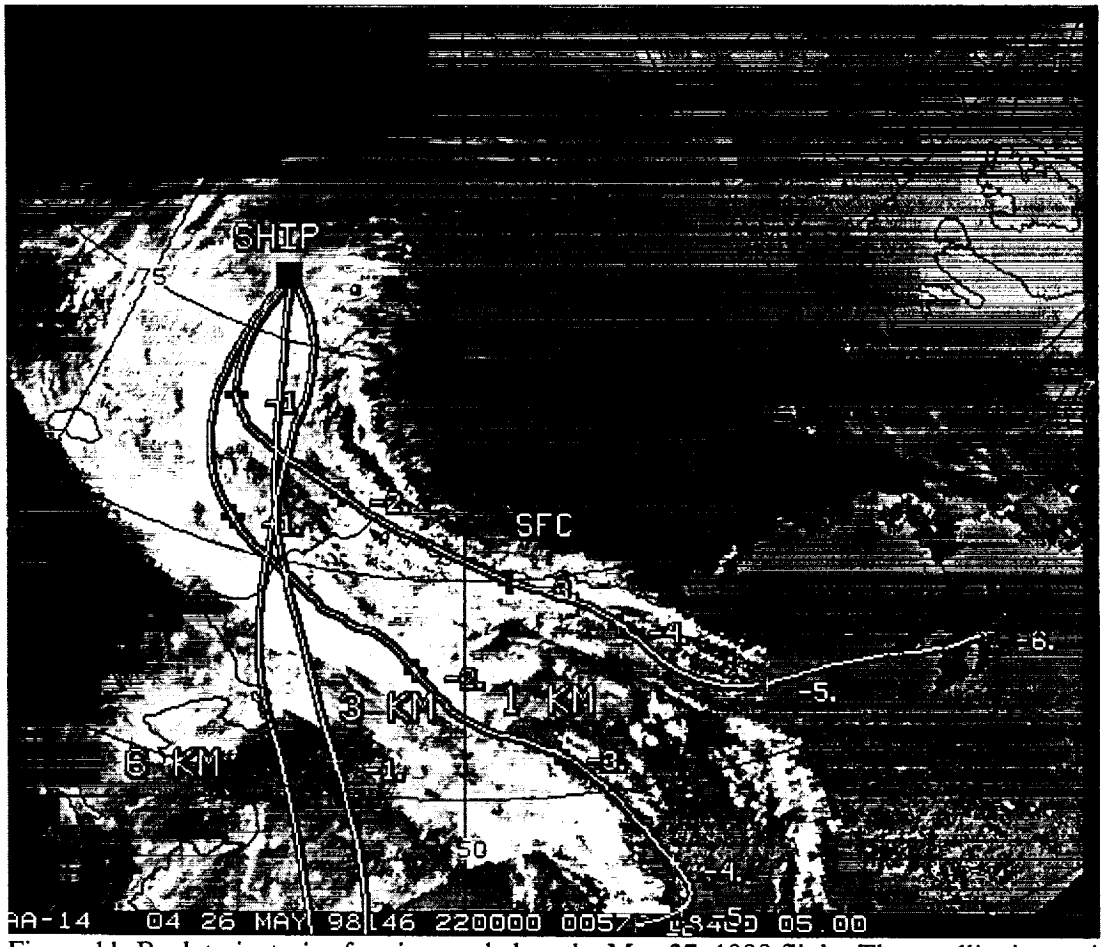

Figure 11: Back trajectories for air sampled on the May 27, 1998 flight. The satellite image is from 1 day prior to the flight.